

1 ***Transport of dissolved Si from soil to river: a***
2 ***review***

3 Benedicta Ronchi, Floor Vandevenne, Ana Lúcia Pena Barão, Wim Clymans, Eric
4 Struyf, Okke Batelaan, Alain Dassargues, Gerard Govers

5 *Benedicta Ronchi, Wim Clymans, Okke Batelaan, Alain Dassargues, Gerard*
6 *Govers*

7 *Earth and Environmental Sciences, K. U. Leuven, Celestijnenlaan 200E 2410,*
8 *3001 Heverlee, Belgium*

9 *Floor Vandevenne, Ana Lúcia Pena Barão , Eric Struyf*

10 *Ecosystem Management Research Group, Department Biology, University*
11 *Antwerp, Campus Drie Eiken, D.C.116, Universiteitsplein 1, 2610 Wilrijk,*
12 *Belgium*

13 *Okke Batelaan*

14 *Department of Hydrology and Hydraulic Engineering, Vrije Universiteit Brussel,*
15 *Pleinlaan 2, 1050 Brussels, Belgium*

16 *Alain Dassargues*

17 *Hydrogeology and Environmental Geology, Dept. of Architecture, Geology,*
18 *Environment and Civil Engineering (ArGEnCo) and Aquapole, Université de*
19 *Liège, B.52/3 Sart-Tilman, BE-4000 Liège, Belgium.*

20 **Abstract**

21 This paper reviews the processes which determine the concentrations of dissolved silicon (DSi) in
22 soil water and proposes a mechanistic model for understanding the transport of Si through a typical
23 podzol soil to the river. DSi present in natural waters originates from the dissolution of mineral
24 and amorphous Si sources in the soil. However, the DSi concentration in natural waters will be
25 dependent on both dissolution and deposition/precipitation processes. The net DSi export is
26 controlled by soil composition like (mineralogy and saturated porosity) as well as water
27 composition (pH, concentrations of organic acids, CO₂ and electrolytes). These state variables
28 together with production, polymerization and adsorption equations constitute a mechanistic
29 framework determining DSi concentrations. For a typical soil profile in a temperate climate, we
30 discuss how the values of these key controls differ in each soil horizon and how it influences the
31 DSi transport. Additionally, the impact of external forcings such as seasonal climatic variations
32 and land use, is evaluated. This model is a first step to better understand Si transport processes in
33 soils and should be further validated with field measurements.

34

35 *Keywords: Si transport; model; land use; biogenic Si*

36

37 1. Introduction

38 In aquatic systems, dissolved Si (DSi) is an important nutrient. Dissolved Si is mainly delivered to
39 the oceans by river discharge: rivers provide more than 80% of the total input of dissolved silicon
40 (DSi) into the oceans [136], the rest being provided by aeolian dust input and ocean floor
41 weathering. Given the relatively low residence time of DSi in the ocean reservoir (ca. 400 yrs,
42 [136]), the delivery of riverine to the oceans is critical for maintaining primary productivity in the
43 world oceans and plays a crucial role in the biological uptake of CO₂ through the so-called
44 biological carbon pump [76].

45 Land-river Si fluxes depend on the relative contribution of different Si sources and on the type of
46 processes (e.g. biological, physico-chemical, pedological) occurring along the pathway [125, 32].
47 The particulate Si fraction in soils and bedrock consists of well-crystallized minerals (e.g. quartz,
48 other primary and secondary silicates) and amorphous Si (ASi) [119, 32]. ASi can be subdivided
49 in biogenic silica (i.e. plant Si bodies called phytoliths) and non-crystalline inorganic Si fractions
50 (i.e. formed by pedogenic processes). In most ecosystems the biogenic constituent is the most
51 abundant. These ASi fractions are important for Si delivery: (i) they can be up to 17 times more
52 soluble than quartz [54] and their dissolution may therefore constitute the most important source of
53 DSi delivered to rivers by groundwater and/or surface and subsurface runoff [62] and (ii) ASi may
54 be directly delivered to aquatic systems by physical erosion during erosion events [124, 22].

55 Thus, DSi concentrations in rivers will to a large extent be controlled by DSi concentrations in
56 soil pore water. DSi concentrations in soil water will have an important effect on DSi
57 concentrations in and DSi delivery to rivers: several studies have shown during large runoff events
58 often consists for a large part of soil pore water that is pushed out of the soil system by the new
59 precipitation. Understanding the mechanisms controlling DSi dynamics within soils is therefore
60 key to understanding spatial and temporal variations in river water and, hence, in Si delivery to
61 the ocean.

62
63 A wide range of processes other than dissolution control soil pore water DSi concentrations:
64 adsorption on Fe- and Al-oxides, polymerization, formation of nanocolloids, precipitation of
65 secondary minerals and uptake by vegetation [41, 137, 32, 98, 2778] which complexes the
66 comprehension of land-river Si transfer. These processes are described separately by physically
67 based equations but models combining all processes do not yet exist. Such a model should not
68 only consider soil processes but should account for the effects of vegetation as vegetation
69 profoundly affects the intensity of the biogeochemical Si cycling [7, 2, 13, 30]. The latter implies
70 that land use may strongly affect DSi delivery, as land use changes will not only affect vegetation
71 but also soil hydrology and soil chemistry. Finally, at the landscape scale, geomorphological and
72 hydrogeological features as these control which ASi and DSi reservoirs contribute to Si delivery at
73 what time. Indeed, the contributions of various reservoirs will not be constant through time but
74 will vary depending on hydrological conditions (moisture status) as well as vegetation dynamics.

75 Si pools and fluxes in landscapes have previously been discussed in the review of Sommer et al.
76 [125]. Street-Perrott and Barker [126] emphasized the importance of coupling the Si and C

77 cycles, while Cornelis et al. [32] focused their review on the impact of the soil-plant system on
78 DSi in weathering-limited and weathering-unlimited environments. While these reviews provide a
79 good overview of the state of the art of our knowledge with respect to Si cycling, they do not
80 discuss how this knowledge can be integrated in a mechanistic modeling framework that might be
81 used to quantitatively predict (changes in) DSi concentrations and fluxes in soils and DSi delivery
82 from soils to rivers. Other catchment studies developed empirical equations to calculate the DSi
83 concentrations in groundwater and soil pore water based on measurements [122, 62]. These are,
84 however, site specific, non-transferable equations.

85

86 In this review, the DSi delivery at soil profile scale from a typical podzol soil to the river is
87 analysed. In contrast to earlier work, we establish a framework of mechanistic equations that may
88 be used to model DSi transport. An overview is given of all equations describing dissolution,
89 adsorption and uptake of Si by plants. We propose these equations to predict expected variations
90 of Si concentrations within soil profiles and discuss which further steps are needed to develop a
91 fully operational model of DSi production and delivery under different land uses. Finally, we
92 discuss how the different processes are affected by land-use and seasonal variations in vegetation
93 for catchments with comparable climate, lithology but covered by grassland, cropland or forest.

94

95

96

97

98 **2. Sources and sinks of Si in soils**

99 **2.1. Typology of Si-particles**

100 Silica is the second most abundant element in the earth crust and is present in different forms. In
101 soils, mineral Si (MSi) is dominant but amorphous Si (BSi) is also present in significant amounts
102 [126] (Figure 1). Mineral silicates can be subdivided in different categories: the primary minerals
103 formed by magmatic crystallization (quartz, feldspars,...) and the secondary minerals developed
104 during soil formation. The secondary phases, concentrated in the clay fraction of soils, can be well
105 crystallized like phyllosilicates [73], micro-crystalline (autigenic quartz, Opal CT, chalcedon) or
106 short-range ordered (imogolite, proto-imogolite, allophane) [45, 144, 94]. Amorphous forms of
107 mineral Si are non-crystalline inorganic particles forming opal-A or volcanic glasses. Amorphous
108 coatings of opal can also cover secondary minerals [98, 19]. Amorphous Si can be of biogenic
109 origin. In this biogenic Si pool, the phytogenic Si (including phytoliths) is the most important
110 component. Phytoliths are formed by plants who take up DSi from the soil solution, which then
111 precipitates as phytoliths in plant roots, stems and leaves/needles. When dead plant material is
112 decomposed, the phytoliths are released to the topsoil. Phytoliths are not the only important form
113 of ASi in soils: sponge spicules, diatoms and testate amoebae are also important components of

114 biogenic Si ([119, 125], especially in wetlands [128] and forests[4]. A classification of all types of
115 Si-particles is presented in Fig. 1.

116 Although atmospheric inputs are low in comparison to other Si fluxes in the soil-plant system they
117 deserve special attention because they are a net source of DSi for the soil-plant system. Aeolian
118 erosion can collect Si-rich dust from soils and potentially transport it to other continental regions
119 or the ocean. As wind forces are very variable regionally and the mineralogical composition of
120 aeolian dust is dependent on the soil of origin, the process is difficult to quantify at larger scales.
121 Atmospheric inputs from aeolian deposition have been estimated to range from 0.04 to 2 kg Si ha⁻¹
122 year⁻¹ for temperate and tropical forests in non-volcanic areas [126]. The spread of volcanic ashes
123 containing ASi in the form of volcanic glass is generally limited to volcanic regions only, but
124 occasionally volcanic dust is dispersed over large areas, depending on the type and magnitude of
125 the eruption as well as on the meteorological conditions at the moment of eruption. ASi input by
126 rainfall is of the same order of magnitude than that by dust deposition: the maximum value found
127 is 3±2 kg Si ha⁻¹ yr⁻¹ [32].

128

129 **2.2. Si dissolution and weathering**

130

131 The dissolution of silicates and amorphous Si generally forms monosilicic acid (H₄SiO₄; DSi):

132



134 Dissolution can also lead to the formation of polysilicic acid but its stability is relatively low.
135 Depending on pH, temperature and composition of natural waters, depolymerisation of polysilicic
136 acid takes place in a few hours or days[40].

137

138 In contrast to quartz, which is highly ordered, amorphous silica is a short-range order crystal
139 composed of loosely packed silica tetrahedrals. Consequently, the solubility of amorphous silica
140 is much higher (1.8-2mM Si under laboratory conditions) than that of quartz (0.10-0.25mM Si).

141 It is often assumed that the Si concentration in natural waters is mainly controlled by mineral
142 silicate hydrolysis (Equation 1): 45% of the dissolved load in rivers is attributed to mineral (?) Si
143 weathering. [130]. [57, 93, 106115]. The mass-balance for a specific element in an aqueous
144 solution resulting from dissolution of mineral phases can be calculated as follows for for j
145 reactants and p product phases:.

$$146 \sum_{j=1}^i \text{MTC}_p \alpha_p^i = \Delta m_i = m_{i(\text{final})} - m_{i(\text{initial})} \quad (2)$$

147 **Where MTC is the mass-transfer coefficient for any phase (p) in moles, α the stoichiometric**
148 **coefficient of element i in phase p , m the total moles of element i in the initial and final**
149 **solutions [5, 16].** However, the composition of natural waters is not only dependent on mineral

150 composition: dissolution is also influenced by temperature, reactive surface and pH. Si solubility is
 151 relatively constant between pH 2 and 8.5 but increases drastically when pH>9 or pH < 2 (?). Bases
 152 dissolve ASi, imogolite and allophone while acidic conditions enhance the desorption of adsorbed
 153 Si [119]. Gérard et al. [62] take account of the temperature dependency of the Arrhenius equation
 154 (Equation 4) as well as pH when calculating the dissolution rate constant for silicate minerals as
 155 follows:

$$156 \quad r_d = k_d S \{H^+\}^n (1 - e^{-A_r/RT}) \quad (3)$$

$$157 \quad \text{with } A_r = -RT \ln \left(\frac{Q}{K} \right) \quad (4)$$

158 in which r_d is the dissolution rate ($\text{mol kg}^{-1} \text{s}^{-1}$), k_d is the dissolution rate constant ($\text{mol m}^{-2} \text{s}^{-1}$), S is
 159 the reactive surface of the mineral ($\text{m}^2 \text{kgH}_2\text{O}^{-1}$), $\{H^+\}$ is the activity of protons in the reacting
 160 solution, n is an experimental exponent and Q is the ionic activity product of the reaction. The
 161 temperature dependence of k_d is described by

$$162 \quad k_d(T) = k_d^0 e^{-E_a/RT} \quad (5)$$

163 in which k_d^0 is k_d at a given reference temperature, E_a is the apparent activation energy of the
 164 dissolution reaction (kJ mol^{-1}), R is the gas constant ($8.32 \times 10^{-3} \text{ kJ mol}^{-1} \text{ K}^{-1}$) and T is the
 165 temperature (K).

166 The equations above describe the mineral dissolution in deionized water: however, the presence of
 167 electrolytes can increase dissolution rates. Water dipoles attack more easily and efficiently mineral
 168 surfaces on which cations are adsorbed. To correct for this, the Langmuir adsorption model can be
 169 integrated [44] in eq. 4:

$$170 \quad k_d^{corr} = k_d^{Na^+} \sigma_{Na^+} + k_d^{Mg^{2+}} \sigma_{Mg^{2+}} + k_d^{Ca^{2+}} \sigma_{Ca^{2+}} + k_d^0 [1 - (\sigma_{Na^+} + \sigma_{Mg^{2+}} + \sigma_{Ca^{2+}})] \quad (6)$$

$$171 \quad \text{with } \sigma_A = \frac{K_{ad}^A m_A}{1 + K_{ad}^{Na^+} m_{Na^+} + K_{ad}^{Mg^{2+}} m_{Mg^{2+}} + K_{ad}^{Ca^{2+}} m_{Ca^{2+}}} \quad (7)$$

172 Where σ_A is the fraction of sites occupied by cation A, m_A the molal concentration of the cation
 173 and K_{ad}^A the equilibrium adsorption coefficient of the cation. The last term of eq. 6 allows to
 174 account for adsorbed protons on remaining sites as adsorption is a competitive process[66].

175 A further complication is that water acidification by CO_2 production ($P_{CO_2}^m$) and the presence of
 176 organic acids ([org]) also need to be accounted for: [131, 132]:

$$177 \quad r_j = k_H + \frac{\{H^+\}^n}{\{M\}^x \{Al^{3+}\}^y} + \frac{k_{H_2O}}{\{Al^{3+}\}^u} + k_{CO_2} \cdot P_{CO_2}^m + k_{org} [org]^{0.5} \quad (8)$$

178 Where r_j is the dissolution rate of mineral j, k_i is the rate coefficient, M the base cations (Ca^{2+} ,
 179 Mg^{2+} , Na^+ and K^+), n, x, y, u and m apparent reaction orders to be determined experimentally.

180 Similar to eq. 3, the first term of the equation accounts for the effect of pH and solution
 181 composition, but adding this time the effect of Al^{3+} . This term stands for formation and

182 decomposition of activated surface complexes. The concentrations of base cations and Al are pH-

183 dependent: in acid water the base cations on the exchange complex are replaced by H_3O^+ . and
 184 **Al(OH)₃ dissolution is enhanced.** After the replacement of exchange complexes by H_3O^+ , an
 185 alkali-depleted layer enriched in Si and /or Al forms around the mineral. This residual layer will
 186 dissolve slowly. Al therefore has a complex role in the dissolution of minerals as its concentration
 187 is not only pH-dependent (like showed in the first term) but also interacts in the residual layer: t
 188 his interaction is accounted for in the third term of eq. 8. The last two terms calculates the rate
 189 contribution due to the described acidification factors[5].The presence of CO_2 accelerates the
 190 dissolution by providing protons . Berg and Banwart [X] suggest that at neutral to near basic pH
 191 weathering will be enhanced by the reactive carbonate complexes sorbed on mineral surfaces.
 192 Drever and Stillings [46] discussed the effect of organic acids on dissolution rates. Their presence
 193 can significantly increase dissolution rates drive dissolution rates far from equilibrium by
 194 lowering the pH but this process seems only to be significant below pH 5. Pokrovski and Schott
 195 [112] observed that aqueous Si and organic ligands did not easily form complexes. This
 196 observation implies that the adsorption of organic ligands is rather limited to quartz. Drever and
 197 Stillings [46] suggest that organic acids influence the silicate weathering indirectly as secondary
 198 iron and aluminium hydroxides dissolve first. In aluminosilicates the Al-O bounds will break more
 199 rapidly than the stronger Si-O bounds [108,109, 59,37- 39, 103]. The resulting higher permeability
 200 induces an accelerated transport thereby increasing weathering.

201

202 In the equations above water availability is assumed to be non-limiting. However dissolution and
 203 hydrolysis are are only possible by contact between water and minerals. It is therefore logical to
 204 assume that the total weathering amount (?) (R_w) within a soil profile is proportional to the soil
 205 water content (θ) as well as the time (t) of the weathering processes [5]. As the soil composition
 206 and water content vary from one horizon to another, the total weathering rate has to be calculated
 207 for each horizon and finally summed for the whole soil column.

$$208 \quad R_w = \sum_{i=1}^{horizons} \theta_i \sum_{j=1}^{minerals} r_j \cdot t \quad (9)$$

209 It is generally assumed that the weathering processes of silicates are accelerated in the vadose
 210 zone, especially in the root zone where biological activity is more important [3, 134]. This is
 211 mainly due to... However, silicate weathering is also known to increase with increasing
 212 concentrations of the acids H_2CO_3 and H_2SO_4 [87, 83]. These acids are produced in the saturated
 213 zone by mineralization processes of organic compounds and sulfides oxidation respectively [83].
 214 The effect of H_2CO_3 is the same process as observed by Berg and Banwart [X] and is accounted
 215 for in equation 8 by the third term. However, the of H_2SO_4 on Si weathering has hitherto never
 216 been formulated in a similar equation.

217

218

219 The combination of existing knowledge, as presented above, allows us to propose a new set of
 220 equations to approximate the amount of Si dissolved in soil from a diverse range of sources:

221

222

$$223 \quad r_{d \text{ total}} = \sum_{j=1}^{\text{horizons}} (\theta_j \sum_{i=1}^{\text{soil comp}} \alpha_i r_{d_i}) \quad (10)$$

224

$$225 \quad r_{d \text{ hor}} = \theta \sum_{i=1}^{\text{soil comp}} \alpha_i r_{d_i} \quad (11)$$

$$226 \quad r_{d_i} = k_d^{\text{corr}} S\{H^+\}^n (1 - e^{-A_r/RT}) \left(\frac{k_{H_2O}}{\{Al^{3+}\}^u} + k_{CO_2} \cdot P_{CO_2}^m + k_{org}[org]^{0.5} + k_{SO_4^{2-}}[SO_4^{2-}]^a \right)$$

227

(12)

228

$$229 \quad \text{With } k_d^{\text{corr}} = \left(\sum \sigma_A k_d^A \right) + k_d^0 [1 - (\sum \sigma_A)] \quad (13)$$

230 Where A = Na⁺, Ca²⁺, Mg²⁺, K⁺ and Al³⁺. Knowing the *fraction* of each soil component in the soil

231 (α in %), a weighted rate $r_{d \text{ hor}}$ can be calculated for each soil horizon j . The $r_{d \text{ total}}$ is the rate for

232 a whole soil profile. These deterministic equations can be used to calculate the weathering and

233 mobilization potential of DSi to soil water as they are based on known processes affecting the Si

234 dissolution rate. Using deterministic equations is a precise but time-consuming approach since a

235 lot of parameters need to be known (e.g. precise soil and water compositions, precise data base of

236 k_d^0).

237

238

239

240 . As k_d^0 is different for each source type, r_d has to be calculated for each Si soil component i (r_{d_i}),

241 in other words for each mineral.

242

243 Current approaches modeling DSi dynamics generally ignore the biogenic and pedogenic Si pools
244 as potential DSi sources and/or DSi sinks. This strongly contrasts with available field evidence:

245 BSi was found to be the principal DSi source in leaching water and stream water in different areas
246 [52, 64]. The few studies that have been realized on the reactivity of BSi show complex

247 dissolution rates. Saccone et al. [118] tested different Si extraction techniques and concluded that

248 phytoliths dissolve more easily in alkaline solutions while adsorbed and mineral Si were

249 extractable with acid solutions. The substitution of Si by Al at the surface of BSi particles lowers its

250 reactivity [138]. Loucaides et al. [89] showed a positive correlation between deprotonated silanol

251 (SiO⁻) groups, which are present at the outer surface of phytoliths at pH higher than 2.5-3 and

252 dissolution rates. Given the importance of these processes and the variable composition

253 of the BSi soil pool (phytoliths of different plant species, testae, spicules,...), it can be assumed

254 that there is a large range of BSi reactivities [129]. Future research should investigate if BSi

255 dissolution is influenced by similar parameters so that eq. 10 may be possibly extended to include

256 BSi dissolution and reprecipitation of this Si as ASi.

257

258

259 **2.3. Sinks of DSi**

260 Si is not only released in the water of natural systems but it can also: (1) be adsorbed to soil
 261 components; (2) form nanocolloids by polymerization; (3) take part in neoformation and
 262 precipitation as secondary minerals; and (4) actively be precipitated in vegetation as phytoliths.

263 (1) Monosilicic acid (H_4SiO_4) sorbs on solid phases, mainly on Fe- and Al-oxides and hydroxides.
 264 The amount of adsorbed Si increases when pH increases from 4 to 9 [9, 98, 40] and can be
 265 quantified with a charge distribution model[70]. Thermodynamically the adsorption can be
 266 calculated as:

$$267 \quad \left(\frac{\delta \log C_{Si-tot}}{\delta pH} \right)_{\Gamma_{Si}} = \left(\frac{\delta \Gamma_H}{\delta \Gamma_{Si}} - n_H \right)_{pH} \equiv (\chi_H - n_H)_{pH} \quad (14)$$

268 in which $\left(\frac{\delta \log C_{Si-tot}}{\delta pH} \right)_{\Gamma_{Si}}$ is the ratio between the change of the total concentration of DSi (C_{Si-tot})
 269 and the change of pH at a constant silicate loading, Γ_{Si} ; $\frac{\delta \Gamma_H}{\delta \Gamma_{Si}}$ is the ratio of change of the proton
 270 adsorption over the change of the silicate adsorption; n_H is the proton balance in the solution and
 271 χ_H is the proton co-adsorption ratio. Equation 14 implies that the concentration change is equal to
 272 the change in H^+ adsorption (Γ_H) as result of the adsorption of Si at the surface (Γ_{Si}) at a given
 273 constant pH after correction for the mean relative number (n_H) of protons present on the species in
 274 solution at that pH. The n_H and Γ_H are calculated for the chosen reference species of DSi,
 275 $H_4SiO_4^0$. This is the most common species at pH below 9, which means $n_H = 0$ when the pH < 9.
 276 If $H_3SiO_4^{-1}$ is the only Si species present in significant concentration at pH > 9 values n_H will be
 277 equal to -1 [71, 114].

278(2) Monosilicic acid ($H_4SiO_{4(monon)}$) forms critical nuclei that rapidly develop into nanocolloids
 279 ($H_4SiO_{4(nano)}$) by oligomerization. Polymerisation of these oligomers takes place in acidic and
 280 neutral environments ($2 < pH < 7$). Monosilicic acids are negatively charged at higher alkalinity
 281 values. Electrostatic forces then prevent polymerization except when the presence of metal cations
 282 allows to neutralize the monomers. If the nanocolloids aggregate or are submitted to processes like
 283 coalescence, SiO_2 precipitates [116, 74, 95, 75] and forms ASi particles. Thus, the relative
 284 amounts of the different types of Si depend on the environmental conditions. In natural
 285 environments, up to 65% of total aqueous silica can be composed of nanocolloidal silica [27].
 286 High amounts of nanocolloidal silica are present in environments with low pH (3-4) and at
 287 neutral pH in combination with a low ionic strength. In acidic environments the concentration of
 288 monomeric Si is in equilibrium with the concentration of nanocolloidal Si. Si precipitation is
 289 rather limited in these conditions in contrast to environments with neutral pH [27]. To simulate the
 290 concentrations of monomeric ($[SiO_{2(monon)}]$) and nanocolloidal SiO_2 ($[SiO_{2(nano)}]$) a
 291 supersaturation model (equations 15 and 16) was proposed by Conrad et al. [27]:

$$292 \quad [SiO_{2(monon)}] = \left(3k_1 t + \frac{1}{([SiO_{2(monon)})_{t=0} - [SiO_{2(eq)}]} \right)^{-1/3} + [SiO_{2(eq)}] \quad (15)$$

293 **And:**

$$294 \quad \frac{d[SiO_2(nano)]}{dt} = \frac{1}{4} k_1 \left[\left(3k_1 t + \frac{1}{([SiO_2(mono)]_{t=0} - [SiO_2(eq)]^3)} \right)^{-1/3} + [SiO_2(eq)] \right]^4 -$$

$$295 \quad k_2 [SiO_2(nano)]^m \quad (16)$$

296 With $[SiO_2(eq)]$ the equilibrium concentration of precipitated amorphous SiO_2 , k_1 is the reaction
297 rate constant for the formation of critical nuclei, k_2 is the rate of precipitation and m is the reaction
298 order with respect to $SiO_2(nano)$.

299 (3) Processes of pedogenic formation of secondary minerals (phyllosilicates, silica and short-range
300 ordered aluminosilicates) depend on DSi concentrations in the soil pore water. High Al
301 disponibility favorises clay formation [91]: under these conditions, Short-range ordered Al-Si
302 compounds (hydroxyaluminosilicates, HAS) are formed in soils with $pH > 5$ [144]. HAS are, an
303 amorphous precursor of imogolite [50, 41]. In presence of active organic matter, the formation of
304 allophane and imogolite is suppressed as Al preferentially forms complexes with organic matter in
305 those conditions. As a consequence, opaline silica precipitates (Huang, 1991). It should be kept in
306 mind that for the precipitation of each secondary mineral, specific equilibrium conditions need to
307 be reached.

308 (4) Plants take up DSi from soil solution especially during the growing season, which can result in
309 a decrease of DSi concentrations during spring and summer [56]. This uptake can be higher (active
310 uptake) than, r proportional to (passive uptake) or lower than (active exclusion) the predicted
311 uptake by water mass transfer. Lower uptake leads to H_4SiO_4 accumulation in the soil. Cornelis et
312 al. [32] reviewed the literature on Si accumulation in plants and showed that both the main source
313 and sink for DSi in soil solutions are phytoliths. Farmer et al. [52] showed that the dissolution of
314 phytoliths stored in soil were the main contributor to DSi in the river water during winter rains and
315 spring snowmelt [52]. However, while there is ample evidence showing that the plant reservoir is
316 important, very little quantitative information is at present available with respect to the relative
317 contribution of biogenic and mineral Si to DSi in soil water for natural and cultural ecosystems.
318 Gérard et al. [63] emphasized this will depend on site-specific conditions.

319 To calculate the active uptake of Si the Michaëlis-Menten (Monod) rate (equation 17) can be used:

$$320 \quad r_a = k_M \left(\frac{[Si]}{K_M + [Si]} \right) \quad (17)$$

321 where r_a is the active uptake of Si ($\text{mol L}^{-1}\text{s}^{-1}$), k_M is the kinetic constant ($\text{mol L}^{-1}\text{s}^{-1}$) and K_M is the
322 half saturation constant (mol L^{-1}). This equation is commonly simplified to a first order rate
323 equation (equation 18) by attributing a very high value to K_M .

324 For passive uptake r_a is equal to:

$$325 \quad r_a = \frac{k_M}{K_M} [Si] \quad (18)$$

326 Which results in a very small value of kM .

327 Active uptake will lower the Si concentration in soil pore water and the DSi concentration in
328 receiving rivers may therefore be expected to decrease during periods of active DSi uptake by
329 terrestrial vegetation.

330 **2.4. Towards an integrated model**

331

332 [Fig. 1 about here]

333 Only a few attempts have been made to simulate the net effect of both sinks and sources on
334 the final DSi concentration in the soil solution and such studies were only carried out for
335 forested environments. Gérard et al. [63] proposed a conceptual model and simulated it using
336 the MIN3P code in which active and passive uptake of Si were integrated. Active uptake was
337 assumed to be important, as there was no evidence for another Si sink.

338 We propose to estimate the Si concentration by coupling all known equations expressing Si
339 dissolution and sink processes (Fig. 2). Firstly, mineral dissolution in a specific soil horizon is
340 calculated by obtaining r_d from equation 10, which is subsequently by the bulk density (ρ), the
341 porosity (ϕ) and the soil moisture (θ) of the soil horizon under consideration. In the case of active
342 uptake, the uptake by vegetation (described by r_a) has to be accounted for in the root zone using
343 eq. ???. The obtained value (r_{net} in $\text{mol L}^{-1} \text{s}^{-1}$) is then multiplied by the duration of a time step (t in
344 s) to obtain the gross increase in DSi concentration, after which losses due to the
345 adsorption/precipitation of Si are estimated using eq. ????. The final Si concentration obtained is
346 the total of the monomeric and nanocolloidal SiO_2 . Estimating the relative importance of both
347 fraction requires that the monomeric SiO_2 is measured, e.g. with the molybdenum blue method
348 [73]. Clearly, this Si model needs to be coupled with a water flux model. This is not only
349 necessary to estimate active uptake but also to simulate Si fluxes between different soil horizons.

350 [Fig. 2 about here]

351

352 Fig. 3 is a schematic representation of a podzol soil system to which our model was applied,
353 whereby passive Si uptake by vegetation is assumed. We assumed steady-state downward
354 water flow at a rate of.... As water is flowing downward through the soil profile, the DSi
355 concentration in particular horizon results from the sum of the DSi concentration measured
356 in the horizon above and the produced or deposited DSi in the considered horizon. In general,
357 the simulated DSi concentration builds up with depth (Fig. 3). The relative importance of the
358 parameters (Table 1) from our model (Fig. 2) depend on the active processes in a specific
359 horizon, hence they needed to be estimated for each horizon. Simultaneous mobilization of Si
360 in the humus layer is expected from the processes: dissolution, transfer with upward
361 capillary movement and uptake by roots and mycorrhizal hyphae. Site specific conditions
362 will determine the relative importance of these mechanisms [64]. The concentration of organic

363 acids, BSi and $p\text{CO}_2$ (equation 12) are probably most important in the humus layer and in the root
364 zone (A horizon) which should lead to a rapid Si dissolution (Fig. 3). For the humus layer of
365 podzolic soils, low molecular weight organic acids (LMWOA) concentrations ranges between
366 0.50145 mM and 2.6445 mM while pH vary between 2.97 and 3.81 and DSi ranges reach 25-353
367 μM [140].

368 The uptake by vegetation is active in the root zone. In Fig. 3 the relative values of DSi is
369 estimated for a soil with passive uptake by vegetation, the DSi concentration in soil water
370 will not be influenced by vegetation ($r_a=0$). In the E-horizon most soluble particles have been
371 leached out and only the most stable minerals are left over, which should lead to no further
372 change in DSi concentration in this horizon (Fig. 3). For podzolic soils, LMWOA
373 concentrations ranged from 0.00 to 0.45084 mM, pH from 2.59 to 4.04 and DSi from 103 to 1032
374 μM in the E-horizon. In the B-horizons of these soils, LMWOA concentrations ranged from 0.00
375 to 0.12455 mM, pH from 4.44 to 6.68 [140]. As the acidity is lower in the B-horizon than in the
376 overlying horizons, parameters $\{H^+\}$ and $[org]$ (equation 12) diminish resulting in a lower
377 dissolution rate (r_{d_i} in equation 12) and in generally lower. Resulting DSi concentrations in soil
378 water are generally lower in the B-horizon (116-351 μM in [140]) than in the E-horizon. In the B-
379 horizon DSi can be adsorbed due to the higher concentration of Al- and Fe-hydroxides
380 (equation 16) and oxides and precipitation of secondary minerals can take place (Fig. 3). The
381 concentrations of Al and base cations (equation 12) are probably the most important in the B
382 horizon. To complicate the situation the presence of organic acids, $p\text{CO}_2$ and BSi needs to be
383 accounted for when root zones extent into the E- and B-layers. In that case concentrations of
384 organic acids and BSi will be higher over a deeper section of the soil profile. Finally, DSi
385 concentrations depend on the importance of each of the processes described. In the upper
386 part of the soil profile the poorly known biological and pedogenic processes probably control
387 the Si-cycle.

388 Deeper in the soil, geological processes (weathering of minerals) are controlling the Si-
389 transport. Those processes are better known. In the saturated area, sulfates and carbonates
390 should be taken into account when using equation 12. In Fig. 3, homogeneous bedrock was
391 assumed.

392 [Table 1 about here]

393 Soil moisture will depend on soil texture: θ will typically range between 0.25-0.45 in silt and
394 between 0.1-0.4 in sandy loam. However storage and retention capacities vary through a soil
395 profile: the clay richer B-horizon have a bigger retention capacity which provides a higher θ values
396 [81]. In this horizon residence time (equation 15) of the water will be higher, which gives
397 more time for all processes to take place. In the capillary fringe located just above the
398 groundwater level, θ increases drastically (Fig. 3) and approximates saturation, e.g. ϕ (Table 1).
399 A higher soil moisture will facilitate dissolution as it occurs when water comes in contact
400 with the solid phases of the soil (equation 9, 10 & 11) as well as DSi diffusion from capillary

401 to leaching pore water. The relative water content profile represents an average situation, in
402 dry or wet conditions the top of the profile certainly differs.

403 [Fig. 3 about here]

404

405

406 **3. Delivery of Si from the soil to the river**

407 The approach to describe DSi mobilization depends on the scale of the study. On a global scale
408 DSi transport depends on lithology and runoff, although vegetation and temperature have been
409 highlighted as potential factors influencing this transport [17, 67,, 79]. This reflects the
410 importance of primary mobilization of Si for the intensity of the Si cycle: even though more and
411 more studies show the importance of the biological pathways, prime mobilization is an important
412 boundary condition for the vegetation and ecosystem filters functioning [129].

413 On the ecosystem scale, general biogeochemical mass balances of Si have been established [15,
414 102]. Processes leading to DSi export are excluded from these models. According to Drever and
415 Stillings [46], transport controls weathering, which process is essentially important in the saturated
416 zone (Fig. 3). Still a lot of different processes appear to influence Si export (Fig. 3). Therefore it is
417 necessary to focus on the different hydrological zones: the unsaturated zone and the saturated
418 zone.

419 The effective transport of the DSi will depend on soil hydraulic parameters like the hydraulic
420 conductivity, the porosity, the bulk density and the matrix tortuosity, dispersivities, effective
421 diffusion coefficient and adsorption partitioning coefficient.

422 Graf and Therrien [66] simulated the transport of DSi with thermohaline groundwater flow at the
423 catchment scale in 3D. Since their focus is on groundwater flow, they only consider saturated
424 ($\theta=1$) conditions and hence neglect plant uptake. They included in their model the effect of
425 adsorption by including a retardation factor. The reactive transport of DSi is expressed in equation
426 18 which assumes fluid incompressibility and constant fluid density[8].

$$427 \frac{\delta(R\phi C)}{\delta t} = \frac{\delta}{\delta x_i} \left(\phi D_{ij} \frac{\delta C}{\delta x_j} - q_i C \right) + \Gamma_m \quad (18)$$

428 In equation 18, i and j are the dimension and equal to 1, 2 or 3, q_i is the Darcy flux ($m s^{-1}$) which
429 depends on the hydraulic conductivity of the soil, C ($kg l^{-3}$) is the solute concentration, R [-] is the
430 retardation factor, D_{ij} ($m^2 s^{-1}$) is the coefficient of hydrodynamic dispersion, Γ_m ($g l^{-3} s^{-1}$) is the
431 source/sink term or the net production of H_4SiO_4 . The coefficient of hydrodynamic dispersion D_{ij}
432 is detailed in Bear's equation (equation 19) [8] where α_l (m) and α_t (m) are respectively the
433 longitudinal and transverse dispersivity, τ is the matrix tortuosity, D_a ($m^2 s^{-1}$) is the free-solution
434 diffusion coefficient and δ_{ij} (-) is the Kronecker delta function. The transport will also be retarded
435 partly due to adsorption. The retardation factor R defined in equation 20[55] depends on the bulk

436 density ρ_b (g m^{-3}) of the porous medium and the equilibrium distribution coefficient K_d ($\text{g}^{-1} \text{m}^3$) for
 437 a linear Freundlich isotherm.

$$438 \quad \phi D_{ij} = (\alpha_l - \alpha_t) \frac{q_i q_j}{|q|} + \alpha_t |q| \delta_{ij} + \phi \tau D_d \delta_{ij} \quad (19)$$

$$439 \quad R = 1 + \frac{\rho_b}{\phi} K_d \quad (20)$$

440 While Graf and Therrien [66] studied the transport of DSi only for the saturated zone, Gérard et al.
 441 [62] investigated processes controlling DSi on the scale of the soil profile, in the unsaturated zone.
 442 The DSi concentrations were measured in leachates and in capillary solutions. The seasonality in
 443 DSi differed between capillary solutions and leaching solutions, maximum DSi values were
 444 observed in different seasons. The DSi concentrations in capillary solutions were mainly
 445 controlled by surface weathering. This aqueous Si diffuses then slowly to leaching solutions.
 446 Gérard et al. [62] suggest that diffusion goes more rapidly in well drained systems, like those
 447 studied by Berner et al.[12]. In Gérard et al. [63] the flux is simulated based on equation 21 through
 448 the first 120 cm of a topsoil covered by a forest. In this zone and on this scale the uptake flux (q_p
 449 [s^{-1}]) of the solute (C [$\text{mol l}^{-1} \text{s}^{-1}$]) by vegetation will have an influence on the Si transport. The soil
 450 moisture is also taken into account here as the topsoil is located in the partially saturated zone and
 451 since transport can only take place if enough water is available. For the 1D simulation of Si flux
 452 through vertical soil profiles, the equation for the hydrodynamic dispersion coefficient D_{ij}
 453 (equation 19) has been simplified (equation 22). Retardation is not taken into account in this model
 454 since previous research in the same study area pointed out the larger importance of diffusive
 455 processes [62].

$$456 \quad \frac{\delta(\theta \phi C)}{\delta t} = \frac{\delta}{\delta x_i} \left(\theta \phi D_{ij} \frac{\delta C}{\delta x_j} - q_i m \right) + \Gamma_m - q_p C \quad (21)$$

$$457 \quad D_{ij} = (\alpha_l - \alpha_t) q_i + D_d \quad (22)$$

458 Here, we showed that the scale of the study and the zone of interest have determined the choice of
 459 parameters. To simulate all processes in a catchment we would have to combine equations 18 and
 460 21 and use equation 23. In the partially saturated zone, θ is lower than 1 as opposed to the
 461 saturated zone where it is equal to 1. The q_p will be higher than 0 in the root zone in contrast to the
 462 zone below the roots where it is equal to 0. For the hydrodynamic dispersion coefficient D_{ij} it is
 463 recommended to use equation 19, at least if all parameters can be estimated.

$$464 \quad \frac{\delta(\theta R \phi C)}{\delta t} = \frac{\delta}{\delta x_i} \left(\theta \phi D_{ij} \frac{\delta C}{\delta x_j} - q_i m \right) + \Gamma_m - q_p C \quad (23)$$

465 For the soil profile illustrated in Fig. 3, we propose a model as presented in Fig. 4. The DSi is
 466 calculated for each soil horizon. The relative importance of the internal processes of each horizon
 467 are illustrated by the thickness of the internal arrows. The water flows with the calculated
 468 transported concentrations (equation 23) from one horizon to another as illustrated by the dashed
 469 arrows. While the saturated zone is assumed to have a homogeneous lithology the DSi

470 concentrations calculated in the final box should be similar to the DSi concentrations in the river
471 during base flow. Here the transport equation 23 is also used with θ equal to ϕ .

472 [Figure 4 about Here]

473 **4. External forces altering internal dynamics**

474 **4.1. Effect of land use**

475 Land use has an impact on different parameters of the soil-vegetation continuum (soil structure,
476 vegetation, hydrology, etc.) and will impact Si dynamics in ecosystems. Evidently, Si export
477 fluxes from different ecosystems vary significantly [127, 49, 105]. To take into account the role of
478 ecosystem as filter in the Si transport [129], we show for the three most common temperate land
479 use types (croplands, forest and grasslands/pastures) how DSi concentrations and controlling
480 parameters (equation 12) are influenced by land use (Fig. 5). Most research has focused on Si-
481 cycling of tropical and temperate forests [2, 7,56, 63, 26, 22]. Few studies have been realized in
482 grasslands [13, 96, 99] and almost no study [110, 124] deals with Si dynamics in cropland
483 ecosystems.

484 Weathering rates and the internal biogeochemical cycle of Si depend on the type of vegetal cover
485 (quality and quantity of roots), biomass and litter, which differ from one land cover to another.
486 Plants change soil physical properties by binding fine particles and disintegrating bedrock which
487 alters the surface area and the interaction time between minerals and water. Consequently,
488 chemical weathering rates, root exudates and cation biocycling increase with plant development
489 [84, 10, 4882]. Soil temperature and the susceptibility to erosion depends also on the vegetation
490 cover. Finally, vegetation will have an impact on the chemical properties of the soil solution. The
491 plants and associated microbiota generate chelating ligands and acidifying products like CO₂ and
492 organic acids. Roots take up chemical elements that partly and delayed come back to the soil by
493 degradation of the litter [24, 102, 15, 28, 47, 141]. Hence, land use management will disturb the
494 natural Si-geobiocycling.

495 Forests have a thick humus layer covering the root penetrated soil profile. Litterfall restitutes large
496 amounts of biologically precipitated Si to the soil system. This implies an increased availability (or
497 large pool) of easily dissolvable Si. Consequently, DSi concentrations are high (last column of Fig.
498 5), e.g. 375±126µM in soil water and 423±52 µM in river water at base flow [23]. Forests soils are
499 typically acidic but still differ between tree-stand compositions, e.g. pH is lower in coniferous
500 forests than in deciduous forests (Johansson et al., 2003). The thick humus layer will also provide
501 organic acids and dissolved organic matter to the soil solution[111], which enhances the
502 dissolution of Si (equation 12). Moreover, uptake of DSi is quite important, although it is not
503 proven that this is an active process in forests [31]: r_A was thus neglected for forests in Fig. 5. In
504 comparison to their DSi losses, forests are characterized by an important internal biogeochemical
505 (re-)cycling of Si [2, 91,100]. In temperate forests, vegetation uptake ranges from 2.3 to 43 kg ha⁻¹
506 yr⁻¹, Si restitution by litterfall ranges from 2.1 to 41 kg ha⁻¹ yr⁻¹, while the export by drainage from

507 the catchments ranges only from 0.7 until 28 kg ha⁻¹ yr⁻¹ [7, 30, 97, 63]. Due to this intensive
508 internal cycling, the transport of DSi towards the river is delayed [25]. BSi preservation in forest
509 soils has been shown for different climates, the stable BSi pool represents an accumulation rate 4
510 to 6 kg Si ha⁻¹yr⁻¹ in equatorial rainforests [2] and 0-1 kg Si ha⁻¹yr⁻¹ [7] in temperate deciduous and
511 coniferous forest. Weight percentages of ASi determined for a forest soil reached 0.5-1.4% in the
512 humus layer (pH 3.8), 0.3-0.6% in the topsoil and 0.3-0.4% at 30 to 45 cm depth (pH 4.5). Soil
513 water from topsoil had a pH of 4.12-5.05 and concentrations of dissolved organic carbon of 23.5-
514 69.0 mg/l resulting in DSi concentrations of 30.6-64.5 μM. At 60 cm depth, soil water had a pH of
515 4.75-5.52 and concentrations of dissolved organic carbon of 2.3-3.7 mg/l resulting in DSi
516 concentrations of 60.2-80.8 μM at 60 cm depth [29]. Fig. 5 illustrates similar trends trough the soil
517 profile: a parallel decrease for ASi and organic acids as well as an increase of pH and DSi with
518 depth.

519 Soil profiles of grasslands are characterized by shallow roots and a humus layer. Grasses
520 accumulate Si actively, this means Si uptake is larger than water uptake [92]. The biological Si
521 cycling in grasslands is more or less comparable with the biocycling of forests. However, the Si
522 biocycling has greater impact on mineral weathering in grasslands than in forests [13]. The amount
523 of soil phytoliths diminishes like soil organic C with depth (Fig. 5). Blecker et al.[13] measured in
524 different topsoils 0.2-0.5 g cm⁻² soil organic C and 0.1-0.5 g cm⁻² phytoliths. For the same soils at
525 70 cm depth, both parameters were ≤0.1 g cm⁻². The storage of BSi in grassland soils is relatively
526 high compared to forests and varies from 4 to 16 kg Si ha⁻¹yr⁻¹. Different causes have been
527 proposed for this relatively low bio recycling. Climatic weathering could be more important in
528 forests enhancing dissolution processes [13]. The lower specific surface of phytoliths could also
529 explain the lower solubility (10-15 times) of grass BSi in comparison to forest BSi[148]. Due to
530 intensive mowing, and possibly cattle grazing of grasslands, a part of the BSi pool is removed
531 from the ecosystem [127]. In this case, the ASi accumulation in the soil will not be replenished (or
532 restituted) by plant uptake, which could eventually result in depletion of easy dissolvable Si pool.
533 In contrast it has also been shown that grazing can lead to higher BSi in grasses [96, 99].
534 Resulting DSi concentrations in natural waters are rather low compared with forest (last column in
535 Fig. 6), e.g. 108±50μM in soil water and 183±37μM in river water [23].

536 In croplands, harvesting, erosion and the use of fertilizers can lead to Si-depletion in soils. For
537 some specific tillage technique, roots are only present in growing season and are absent during
538 winters due to harvesting. Harvesting prevents litter accumulation and the development of a humus
539 layer which leads to low BSi accumulation in cropland soils [101,; 110, 139]. Erosion is important
540 in croplands as bare soils are exposed to the wind and precipitation. Soil erosion can be especially
541 high during peak-events leading to the removal of ASi from the soil. As a result, dynamics of DSi
542 and ASi in river water of cultivated first-order catchments differ between peak flow events and
543 baseflow[124]. Resulting DSi concentrations in soil water are rather low, e.g. 106±41 μM and
544 204±63μM for different sites[23]. The use of nitrate fertilizers enhances the weathering of Si as
545 nitrification processes releases acids[53].

546 Fig. 5 summarizes the general processes influencing the DSi concentrations for each type of land
547 use. Soil temperature is generally lower under forest than under grassland cover. Cropland soils
548 have higher temperatures and seasonal variations are more important compared to the other land
549 uses [135, 120]. As the measured temperature differences between cropland, grassland and forests
550 are in the order of magnitude of a few degrees (°C), these differences will probably not influence
551 directly the dissolution of Si but can influence biological activity and thus the uptake of DSi, the
552 amount of organic acids, pCO₂, etc. In general the pH is lower in forests than in grasslands and
553 arable lands. The amount of dissolved organic matter is the highest in forests and lower in
554 croplands than in grasslands. The pCO₂ in soils was proved to be the highest in arable land,
555 followed by grasslands and lowest in forests [1]. The acidity parameters (equation 12) driving
556 dissolution are thus different following the land use: in forests organic acids and pH are important
557 but in grassland and cropland pCO₂ will be more important compared to forests.

558

559 [Fig. 5 about here]

560 **4.2. Seasonal climatic variation**

561 Seasonal variations of DSi have been observed in water of temperate forested catchments with
562 humid winters and dry summers ([88, 105]. In summer, rainfall events are typically more
563 intensive. Various explanations are given for the temporal variation in DSi transport [113, 56,105].
564 If lithology of the aquifer varies vertically, more weatherable layers can be in contact with high
565 groundwater levels and release Si, in which case water chemistry can be correlated with
566 groundwater level [113]. The decrease of DSi in natural waters during the growing season can be
567 explained by the DSi uptake by vegetation [56] or by the consumption of DSi by diatoms in the
568 river [105]. In the first case the decrease will be observed in soil waters in contrast to the second
569 case where the decrease is only observed in river water. Gérard et al. [62] observed a significant
570 seasonal variation in soil water and connectivity between the soil and river system: DSi
571 concentrations in capillary soil solutions were generally ca 35 µM lower during winter than during
572 summer.

573 The autumn-winter period characterized by:

- 574 - low evapotranspiration rates which induces low uptake of DSi by passive vegetation,
575 illustrated by a weak interaction for forest and grassland or no interaction in cropland in
576 Fig. 6;
- 577 - higher soil moistures (θ in Fig. 6) and groundwater levels which can enhance dissolution
578 of the lithologies (equations 9, 10, 11);
- 579 - decaying organic matter releasing BSi into the soil giving a larger fresh ASi stock
580 available, especially in forests where litterfall is important (BSi in Fig. 6);
- 581 - polymerization of DSi and complexation of Si with particulate material when water
582 freezes [133].

583 During spring and summer, other processes are important:

- 584 - higher evapotranspiration rates, which induces dryer soils and higher uptake of DSi by
585 vegetation, illustrated as important interaction in Fig. 6 ;
586 - lower soil moistures (θ in Fig. 6) and lower groundwater levels (equations 9,10, 11)
587 limiting unsaturated transport of DSi to the aquifer [23];
588 - higher temperatures increases biological activity which leads to more acid production (pH
589 or H^+ , [org] and pCO_2 in Fig. 6 and equations 6, 7, 8 & 12);
590 - higher acid production results in Si desorption and in a shift of cation exchange equilibria,
591 i.e. base cations are replaced by H^+ on the mineral surfaces (equations 6, 7, 8 & 12) [12].

592 To conclude, DSi concentrations should generally be lower during winter than during summer as
593 acid production will drive a lot of processes enhancing Si dissolution. Transport processes in the
594 dry summer will be slower: maximal DSi concentrations can be observed at different times in soil
595 capillary soil water, leaching solution and river water due to diffusion processes from capillary to
596 leaching solution [62] or due to a long transport time from soil to river.

597 [Fig. 6 about here]

598 **5. Discussion and conclusions**

599 This review presents a conceptual model for DSi transport from landsurface, through each soil
600 horizon of a typical podzol soil, subsurface until the river for catchments with temperate climate.
601 This is the first time a framework of equations is proposed that may be used as a first step to
602 develop a mechanistic model for DSi production and transport. The proposed model needs to be
603 validated by applying the model on fields. As each field has its own specific characteristics, the
604 user of such an equation framework can check which controlling processes and rate limiting
605 processes are important in his study case. Based on that analyse the user can simplify the
606 framework by dismissing some processes, if needed. Still several unknowns need to be further
607 clarified to entirely understand the Si-cycle. On the scale of the soil profile, not all pedogenic
608 processes are known. The influence of sulfates in the saturated zone have been observed in
609 some study cases [83,87] and should be better studied to determine if it is an important
610 process or not. The influence of microbial activity on mineral changes seems difficult to quantify.
611 The reactivity of BSi particles in soil profiles have not been well studied, i.e. is BSi reacting like
612 mineral Si to pH changes?

613 By analyzing the parameters driving DSi production (equation 12), we could state seasonal
614 variation of DSi export is linked to the importance of biological activity. Si-cycling is more
615 important during spring and summer due to high biological activity inducing for example higher
616 acidity production. This results in lower DSi concentrations in soil water during autumn and
617 winter compared to spring and summer.

618 The BSi storage, the Si-cycling and Si-export differs for the three types of land uses (forest,
619 cropland, grassland). It results in high DSi concentrations in the forest rivers. Following the
620 analysis of controlling parameters (section 4.1.), relatively high concentrations are expected in

621 grasslands and low concentrations in croplands due to the respectively decreasing BSi storage and
622 soil acidity. Nevertheless the data from Clymans [23] show no significant difference between DSi
623 in soil water of grassland and cropland. Moreover, the comparison of soil water DSi in different
624 catchments with the same land use [23] show different DSi concentrations. This emphasizes the
625 importance of determining the site-specific parameters influencing the Si transport. On the
626 catchment scale, we emphasized that ecosystem management has an impact on the Si cycle. It is
627 not clear in grazed grasslands how the digestion of grasses influences the availability of BSi to the
628 Si-cycle. Deforestation, harvesting, mowing, grazing retrieve BSi stored in vegetation from the
629 specific ecosystems (forest, cropland or grassland). However the destination of BSi retrieved by
630 deforestation, harvesting and mowing is unknown, it might be released in another Si cycle or not.
631 This is important to figure out for Si-budget calculations on a large scale. However, some
632 parameters (i.e. soil water content, base cations) of our dissolution model are sometimes difficult
633 to compare from one land use type to another as they are influenced by site specific factors
634 (meteorological conditions, soil mineralogy).

635 Struyf et al. [127] proposes a model for the evolution of the Si-cycle and the Si transport during
636 baseflow due to land-use changes. This model proposes an increase in DSi export during the
637 development of a forest, a relatively constant and high export during the climax phase of the forest
638 development. The deforestation will induce a quick increase of Si export [88, 6, 26] on the short
639 term (<20yrs; [26]). Likens et al. [88] supposed the deforestation increased the weathering of
640 primary minerals, but knowing that ASi is much more soluble than primary silicates, Conley et
641 al.[26] proposed three other hypotheses. The excess of DSi can result from the dissolution of ASi
642 contained in cut vegetation left on the soil. Another possible explanation is the mobilization of the
643 large amount of BSi stored in forest soils[25, 13]. The last hypothesis to explain the excess of DSi
644 exported after deforestation is an enhanced leaching due to the re-establishment of vegetation. As
645 the ASi amount diminishes after deforestation the long term evolution (500-1000 yrs; 127) of
646 landscapes from forest to cropland would generate on the long term a diminishing Si export.
647 Clymans et al. [22] observed that historical land use changes resulted in a 50% decrease of BSi
648 storage in Swedish soils. This diminishing Si export can be explained by the change in chemical
649 and physical properties of soils thus by the change in dissolution driving parameters (equation 12).
650 Even if the pH will increase when forest becomes cropland or pasture, the base exchange
651 properties will increase. This could have a lowering effect on DSi concentrations of soil water.
652 Moreover, the decreasing porosity will diminish infiltration capacity and increase erodability [51,
653 117]. As erodability increases, BSi depletion of soils will start.

654 An important question remains: how much DSi exported from out of a catchment comes from BSi
655 relatively to MSi? To understand the relative contribution of the biological filter to eventual
656 output of DSi, Derry et al.[34] combined Ge/Si ratios with the Si concentrations. Cornelis et
657 al. [32] recommended to make a Si mass balance and combine the use of Ge/Si and $\delta^{30}\text{Si}$ as
658 geochemical tracers. These tracers can be used because they are fractionated during the
659 biogeochemical cycle which implies that different sources have different tracer's signatures
660 [109]. Germanium concentrations are relatively high in clayey weathering products compared to

661 concentrations measured in phytoliths [104, 86, 121, 14,33]. The light Si isotopes are
662 preferentially built-in secondary clay minerals, taken up by plants and adsorbed on Fe-oxides. Due
663 to this processes the DSi flowing into the river will be enriched in heavy isotopes [110, 29, 42, 18,
664 36, 35, 60,61] . Si isotopes and element ratios (Si/Mg; Ge/Si) can be good proxies to understand
665 which processes (weathering, uptake by diatoms, uptake by terrestrial vegetation) influence the
666 seasonal variation of DSi in river water [49, 32]. Using these two elements has several advantages:
667 the ratio Ge/Si can be related to the geochemical source of Si and hence sources with similar Si
668 concentration can be differentiated. All these approaches are still in early stages of development,
669 therefore it is presently difficult to assess different Si sources based on either method. Early results
670 are mainly related to small scale isotope fractionation in isolated soil-plant systems, for few
671 species only (Musa sp., bamboo, ...). On the catchment scale, isotope signatures are still difficult
672 to assign, as different biogeochemical mechanisms contribute similarly to isotope ratios. More
673 detailed research on these tracers in specific land use types could significantly enhance this
674 research.

675

676 To assess CO₂ consuming processes like Si weathering [20] or diatom uptake, the exact
677 quantification of the total amount of Si in soils and total amount of DSi transported from the
678 continent to the ocean are essential. In contrast to our proposed model, current approaches
679 (e.g.[65]) ignore the biogenic Si pool as a DSi source, DSi sinks like Si uptake by plants or Si
680 nucleation and differences due to the land use types. Prediction models of global DSi transport in
681 the future will have to take these factors into account as well as the expansion of agriculture
682 (Gordon et al., 2008) and the rising number of peak events due to climate change. Transport of
683 DSi from soil to river will probably diminish in the future. In this study only three land uses were
684 analysed. In urban areas, the Si transport needs to be tackled in a different way, anthropogenic
685 point sources (industries) need to be taken into account and as exposed soil is rather scarce, raw
686 materials will be sources of Si during runoff events [123].

687 To tackle the eutrophication problem the Si:N:P ratios should be considered in order to obtain the
688 whole picture. Eutrophication is due to increasing N and P concentrations, while Si concentrations
689 would not change [21]. Snowmelt periods need to be analysed carefully as DSi can be diluted in
690 rivers during snowmelt periods while nitrates increase enhance eutrophication [68, 69, 149]. Since
691 we discussed the shifts of DSi transport by land-use changes and these changes can affect also the
692 leaching of N [51], the impact of land use changes on the Si:N:P should be further analysed.

693

694 **Aknowledgements**

695 Benedicta Ronchi and Wim Clymans would like to thank the Flemish Agency for the promotion of
696 Innovation by Science and Technology (IWT) for funding them personal promotion grant. Eric
697 Struyf acknowledges FWO (Flemish Research Foundation) for funding his postdoc grant. We
698 acknowledge FWO for funding project “Tracking the biological control on Si mobilization in
699 upland ecosystems” (Project nr. G014609N). Floor Vandevenne and Ana Lúcia Pena Barão would
700 like to thank BOF-UA for PhD fellowship funding.

701

702

703

704 References

- 705 [1] Albertsen M (1977) Labor- und Felduntersuchungen zum Gasaustausch zwischen
706 Grundwasser und Atmosphäre über natürlichen und verunreinigten Grundwässern.
707 Thesis, Univ. Kiel.
- 708 [2] Alexandre A, Meunier J-D, Colin F, Koud J-M (1997) Plant impact on the
709 biogeochemical cycle of silicon and related weathering processes. *Geochim Cosmochim*
710 *Ac* 61-3: 677-682
- 711 [3] Andrews J, Schlesinger W (2001) Soil CO₂ dynamics, acidification, and chemical
712 weathering in a temperate forest with experimental CO₂ enrichment. *Global Biogeochem*
713 *Cy* 15:149-162
- 714 [4] Aoki Y, Hoshino M, Matsubara T (2007) Silica and testate amoebae in a soil under pine-
715 oak forest. *Geoderma* 142(1-2): 29-35
- 716 [5] Appelo CAJ, Postma D (1993) *Geochemistry, Groundwater, and Pollution*. A.A.
717 Balkema, Rotterdam.
- 718 [6] Bailey SW, Buso DC, Likens GE (2003) Implications of sodium mass balance for
719 interpreting the calcium cycle of a northern hardwood ecosystem. *Ecology* 84: 471-484
- 720 [7] Bartoli, F (1983) The biogeochemical cycle of silicon in two temperate forest ecosystems.
721 *Environ Biogeochem Ecol Bull* 35: 469-476.
- 722 [8] Bear J (1988) *Dynamics of fluids in porous media*. Elsevier, New York
- 723 [9] Beckwith RS, Reeve E (1962) Studies on Soluble Silica in Soils. I. The Sorption of silicic
724 acid by soils and minerals. *Aust J Soil Res* 1 (2): 157 - 168
- 725 [10] Berner RA (1992) Weathering, plants and the long-term carbon cycle. *Geochim*
726 *Cosmochim Ac* 56: 3225-3231
- 727 [11] Berner RA (1995) Chemical weathering and its effect on the atmospheric CO₂ and
728 climate In: *Chemical weathering rates of silicate minerals*, Reviews in mineralogy,
729 Mineralogical Society of America, Washington, DC
- 730 [12] Berner RA, Rao JL, Chang S, O'Brien R, Keller CK (1998) Seasonal Variability of
731 Adsorption and Exchange Equilibria in Soil Waters. *Aquat Geochem* 4: 273-290
- 732 [13] Blecker SW, McCulley RL, Chadwick OA, Kelly EF (2006) Biologic cycling of silica
733 across a grassland bioclimate sequence. *Global Biogeochem Cy* 20,
734 DOI:10.1029/2006GB002690
- 735 [14] Blecker SW, King SL, Derry LA, Chadwick OA, Ippolito JA, Kelly EF (2007) The ratio
736 of germanium to silicon in plant phytoliths: Quantification of biological discrimination
737 under controlled experimental conditions. *Biogeochemistry* 86: 189-199
- 738 [15] Bormann BT, Wang D, Bormann FH, Benoit G, April R, Snyder MC (1998) Rapid, plant-
739 induced weathering in an aggrading experimental ecosystem. *Biogeochemistry* 43: 129-
740 155, 1998.
- 741 [16] Bowser CJ, Jones BF (2002) Mineralogical controls on the composition of natural waters
742 dominated by silicate hydrolysis. *Am. J. Sci.* 302: 582-662.
- 743 [17] Bluth GJS, Kump LR (1994) Lithologic and climatologic controls of river chemistry.
744 *Geochim Cosmochim Ac* 58: 2341-2359.
- 745 [18] Cardinal D, Gaillardet J, Hughes H J, Opfergelt S, André L (2010) Contrasting silicon
746 isotope signatures in rivers from the Congo Basin and the specific behaviour of organic-
747 rich waters. *Geophys. Res. Lett.* 37 DOI:10.1029/2010GL043413
- 748 [19] Chadwick OA, Hendricks DM, Nettleton WD (1987) Silica in duric soils, 2. *Mineralogy,*
749 *Soil Sci Soc Am J* 51(4): 982-985.
- 750 [20] Chadwick OA, Kelly EF, Merritts DM, Amundson RG (1994) Atmospheric Carbon
751 Dioxide Consumption During Soil Development. *Biogeochemistry* 24 115-127.
- 752 [21] Cloern JE (2001) Our evolving conceptual model of the coastal eutrophication problem.
753 *Mar Ecol-Prog Ser* 210: 223-253.
- 754 [22] Clymans W, Struyf E, Govers G, Vandevenne F, Conley DJ (submitted) Anthropogenic
755 impact on biogenic Si pools in temperate soils. *Biogeosciences*
756 <http://www.biogeosciences-discuss.net/8/4391/2011/bgd-8-4391-2011.pdf>

- 757 [23] Clymans W, Govers G (sup.), Van Rompaey, A. (cosup.), Struyf, E. (cosup.) (2012) Land
758 use related silica dynamics in terrestrial ecosystems. Thesis. KULeuven.
- 759 [24] Cochran MF, Berner RA (1996) Promotion of chemical weathering by higher plants: field
760 observations on Hawaiian basalts. *Chemical Geology* 132: 71-77
- 761 [25] Conley DJ (2002) Terrestrial ecosystems and the global biogeochemical silica cycle.
762 *Global Biogeochem. Cy.* 16(4) 1121, doi:10.1029/2002GB001894, 2002.
- 763 [26] Conley DJ, Likens GE, Buso DC, Saccone L, Bailey SW, Johnson CE (2008)
764 Deforestation causes increased dissolved silicate losses in the Hubbard Brook
765 Experimental Forest. *Glob Change Biol* 14: 1-7
- 766 [27] Conrad CF, Icopini GA, Yasuhara H, Bandstra JZ, Brantley SL, Heaney PJ (2007)
767 Modeling the kinetics of silica nanocolloid formation and precipitation in geologically
768 relevant aqueous solutions. *Geochim Cosmochim Ac* 71: 531-542
- 769 [28] Cookson WR, Osman M, Marschner P, Abaye DA, Clark I, Murphy DV, Stockdale EA,
770 Watson CA (2007) Controls on soil nitrogen cycling and microbial community
771 composition across land use and incubation temperature. *Soil Biol Biochem*
772 39: 744-756
- 773 [29] Cornelis J-T, Delvaux B, Cardinal D, André L, Ranger J, Opfergelt S (2010) Tracing the
774 mechanisms controlling the release of dissolved silicon in forest soil solutions using Si
775 isotopes and Ge/Si ratios. *Geochim Cosmochim Ac* 74: 3913-3924
- 776 [30] Cornelis J-T, Ranger J, Iserentant A, Delvaux B (2010) Tree species impact the terrestrial
777 cycle of silicon through various uptakes. *Biogeochemistry* 97: 231-245
- 778 [31] Cornelis J-T, Delvaux B, Titeux H (2010) Contrasting silicon uptakes by coniferous trees:
779 a hydroponic experiment on young seedlings. *Plant Soil* 336: 99-106
- 780 [32] Cornelis J-T, Delvaux B, Georg RB, Lucas Y, Ranger J, Opfergelt S (2011) Tracing the
781 origin of dissolved silicon transferred from various soil-plant systems towards rivers: a
782 review. *Biogeosciences* 8: 89-112
- 783 [33] Delvigne C, Opfergelt S, Cardinal D, Delvaux B, Andre L. (2009) Distinct silicon and
784 germanium pathways in the soil-plant system: Evidence from banana and horsetail. *J.*
785 *Geophys Res* 114, G02013, doi:10.1029/2008JG000899.
- 786 [34] Derry LA, Kurtz AC, Ziegler K, Chadwick OA (2005) Biological control of terrestrial
787 silica cycling and export fluxes to watersheds. *Nature* 728: 433
- 788 [35] De La Rocha CL, Brzezinski MA, De Niro MJ (2000) A first look at the distribution of
789 the stable isotopes of silicon in natural waters. *Geochim Cosmochim Ac* 64: 2467-2477
- 790 [36] Delstanche S, Opfergelt S, Cardinal D, Elsass F, André L, Delvaux B (2009) Silicon
791 isotopic fractionation during adsorption of aqueous monosilicic acid onto iron oxide,
792 *Geochim Cosmochim Ac* 73: 923-934
- 793 [37] Devidal JL (1994) Solubilité et cinétique de dissolution/précipitation de la kaolinite en
794 milieu hydrothermal. Approche expérimentale et modélisation. Ph. D. Thesis University
795 Paul Sabatier, Toulouse, France.
- 796 [38] Devidal JL, Dandurand JL, Schott J (1992) In Kharaka, Y. K. and Maest, A. S. (eds)
797 *Water Rock Interaction*. A. A. Balkema, Rotterdam.
- 798 [39] Devidal JL, Schott J, Dandurand JL (1997) An experimental study of kaolinite dissolution
799 and precipitation kinetics as a function of chemical affinity and solution composition at
800 150°C, 40 bars, and pH 2, 6.8, and 7.8. *Geochim Cosmochim Ac* 61: 5165-5186.
- 801 [40] Dietzel M (2002) Dissolution of silicates and the stability of polysilicic acid. *Geochim*
802 *Cosmochim Ac* 64 (19): 3275-3281
- 803 [41] Doucet F, Schneider C, Bones S, Kretchner A, Moss I, Tekely P, Exley C (2001) The
804 formation of hydroxyaluminosilicates of geochemical and biological significance.
805 *Geochim Cosmochim Ac* 65 (15): 2461-2467
- 806 [42] Douthitt CB (1982) The geochemistry of the stable isotopes of silicon. *Geochim*
807 *Cosmochim Ac* 46: 1449-1458.
- 808 [43] Dove PM (1995) Kinetic and thermodynamic controls on silica reactivity in weathering
809 environments, in: *chemical weathering rates of silicate minerals*. Mineralogical Society of
810 America and the Geochemical Society, *Rev Mineral Geochem* 31: 235-290
- 811 [44] Dove PM (1999) The dissolution kinetics of quartz in aqueous mixed cation solutions.
812 *Geochim Cosmochim Ac* 63(22): 3715-27.
- 813 [45] Drees LR, Wilding LP, Smeck NE, Senkayi AL (1989) In: Dixon B, Weed SB (eds),
814 *Minerals in Soil Environments*, 2nd edn. Soil Sci Soc Am J, Madison, Wisconsin.
- 815 [46] Drever JI, Stillings LL (1997) The role of organic acids in mineral weathering. *Colloid*
816 *Surface A* 120: 167-181.
- 817 [47] Drever JI, Zobrist J (1992) Chemical-weathering of silicate rocks as a function of
818 elevation in the southern Swiss Alps. *Geochim Cosmochim Ac* 56: 3209- 3216.

- 819 [48] Drever JI (1994) The effect of land plants on weathering rates of silicate minerals,
820 *Geochim Cosmochim Acta* 58 (10): 2325-2332
- 821 [49] Engström E, Rodushkin I, Ingrid J, Baxter DC, Ecke F., Österlund H, Öhlander B (2010)
822 Temporal isotopic variations of dissolved silicon in a pristine boreal river. *Chem Geol*
823 271: 142–152
- 824 [50] Exley C (1998) Silicon in life: a bioinorganic solution to bioorganic essentiality, *J Inorg*
825 *Biochem* 69: 139–144.
- 826 [51] Falkengren-Grerup U, ten Brink DJ, Brunet J (2006) Land use effects on soil N, P, C and
827 pH persist over 40–80 years of forest growth on agricultural soils. *Forest Ecology and*
828 *Management* 225: 74–81
- 829 [52] Farmer VC, Delbos E, Miller JD (2005) The role of phytolith formation and dissolution
830 in controlling. *Geoderma* 127: 71–79
- 831 [53] Fortner SK, Lyons WB, Carey AE, Shipitalo MJ, Welch SA, Welch KA (2011) Silicate
832 weathering and CO₂ consumption within agricultural landscapes, the Ohio-Tennessee
833 River Basin, USA *Biogeosciences Discuss*, 8, 9431–9469
- 834 [54] Fraysse F, Pokrovsky OS, Schott J, Meunier JD (2006) Surface properties, solubility and
835 dissolution kinetics of bamboo phytoliths. *Geochim Cosmochim Acta* 70: 1939–1951.
- 836 [55] Freeze RA, Cherry JA (1979) *Groundwater*. Englewood Cliffs (NJ): Prentice Hall.
- 837 [56] Fulweiler RW, Nixon SW (2005) Terrestrial vegetation and the seasonal cycle of
838 dissolved silica in a southern New England coastal river. *Biogeochemistry* 74: 115–130
- 839 [57] Garrels RM, Mackenzie FT (1967) In: RF Gould (ed) *Advances in Chemistry Series 67*,
840 American Chemical Society, Washington D.C.
- 841 [58] Gordon LJ, Peterson GD, Bennett EM (2008) Agricultural modifications of hydrological
842 flows create ecological surprises. *Trends Ecol Evol* 23(4): 211-219.
- 843 [59] Gautier JM, Oelkers EH and Schott J (1994) Experimental study of K-feldspar dissolution
844 rates as a function of chemical affinity at 150°C and pH 9. *Geochim. Cosmochim Acta* 58:
845 4549–4560.
- 846 [60] Georg RB, Reynolds BC, Frank M, Halliday AN (2006) Mechanisms controlling the
847 silicon isotopic compositions of river waters, *Earth Planet Sc Lett* 249: 290–306.
- 848 [61] Georg RB, Reynolds BC, West AJ, Burton KW, Halliday AN (2007) Silicon isotope
849 variations accompanying basalt weathering in Iceland. *Earth Planet Sc Lett*, 261: 476–
850 490.
- 851 [62] Gérard F, François M, Ranger J (2002) Processes controlling silica concentration in
852 leaching and capillary soil solutions of an acidic brown forest soil (Rhône, France).
853 *Geoderma* 107: 197–226.
- 854 [63] Gérard F, Mayer KU, Hodson MJ, Ranger J (2008) Modelling the biogeochemical cycle
855 of silicon in soils: Application to a temperate forest ecosystem, *Geochimica et*
856 *Cosmochimica Acta* 72: 741–758
- 857 [64] Giesler R, Ilvesniemi H, Nyberg L, van Hees P, Starr M, Bishop K, Kareinen T,
858 Lundström US (2000) Distribution and mobilization of Al, Fe and Si in three podzolic soil
859 profiles in relation to the humus layer. *Geoderma* 94: 249–263.
- 860 [65] Goddés Y, François LM, Probst A, Schott J, Moncoulon D, Labat D, Viville D (2006)
861 Modelling weathering processes at the catchment scale: The WITCH numerical model
862 *Geochim Cosmochim Acta* 70: 1128–1147
- 863 [66] Graf T, Therrien R (2007) Coupled thermohaline groundwater flow and single-species
864 reactive solute transport in fractured porous media *Adv in Water Res* 30: 742–771.
- 865 [67] Hartmann J, Jansen N, Dürr HH, Kempe S, Köhler P (2009) Global CO₂-consumption by
866 chemical weathering: What is the contribution of highly active weathering regions? *Glob*
867 *Planet Change* 69 (4): 185–194.
- 868 [68] Hatano R, Nagumo T, Hata H, Kuramochi K (2005) Impact of nitrogen cycling on stream
869 water quality in a basin associated with forest, grassland, and animal husbandry,
870 Hokkaido, Japan. *Ecol Eng* 24: 509–515.
- 871 [69] Hayakawa A, Nagumo T, Kuramochi K, Hatano R (2003) Characteristics of nutrient load
872 in a stream flowing through a livestock farm during spring snowmelt. *Soil Sci Plant Nutr*
873 49: 301–305.
- 874 [70] Hiemstra T, Barnett MO, van Riemsdijk WH (2007) Interaction of silicic acid with
875 goethite. *J Colloid Interf Sci* 310: 8–17.
- 876 [71] Hiemstra T, Van Riemsdijk WH (2002) in: *Encyclopedia of Surface and Colloid Science*,
877 first ed., Dekker, New York.
- 878 [72] Huang PM (1991) Ionic factors affecting the formation of short-range ordered
879 aluminosilicates. *Soil Sci Soc Am J.* 55: 1172–1180

- 880 [73] Iler, RK (1979) *The Chemistry of Silica: Solubility, Polymerization, Colloid and Surface*
881 *Chemistry, and Biochemistry*. John Wiley & Sons.
- 882 [74] Izumi S, Hara S, Kumagai T, Sakai S (2005). Molecular dynamics study of homogeneous
883 crystal nucleation in amorphous silicon. *J. Cryst. Growth* 274: 47–54.
- 884 [75] Icopini GA, Brantley SL, Heaney PJ (2005) Kinetics of silica oligomerization and
885 nanocolloid formation as a function of pH and ionic strength at 25°C. *Geochim*
886 *Cosmochim Ac* 69 (2): 293–303.
- 887 [76] Ittekkot V, Humborg C, and Schäfer P (2000) Hydrological alterations and marine
888 biogeochemistry: a silicate issue. *BioScience* 50: 777–82.
- 889 [77] Izumi S, Hara S, Kumagai T, Sakai S (2005) Molecular dynamics study of homogeneous
890 crystal nucleation in amorphous silicon. *J. Cryst. Growth* 274: 47–54.
- 891 [78] Jackson ML, Tyler SA, Willis AL, Bourbeau GA, Pennington RP (1948) Weathering
892 sequence of clay-size minerals in soils and sediments. I. Fundamental generalizations. *J*
893 *Phys Colloid Chem* 52: 1237–1260
- 894 [79] Jansen N, Hartmann J, Lauerwald R, Dürr HH, Kempe S, Loos S., Middelkoop H (2010)
895 Dissolved silica mobilization in the conterminous USA. *Chem Geol* 270: 90–109
- 896 [80] Johanson E, Sandén P, Öberg G (2003) Organic Chlorine in Deciduous and coniferous
897 forest soils in Southern Sweden. *Soil Sci* 168 (5): 347-355
- 898 [81] Jury W, Horton R (2004) *Soil Physics*. 6th Edition. John Wiley & Sons New York 390 p.
- 899 [82] Kelly EF, Chadwick OA, Hilinski TE (1998) The effect of plants on mineral weathering.
900 *Biogeochemistry* 42: 21– 53.
- 901 [83] Klaminder J, Grip H, Mörth CM, Laudon H (2011) Carbon mineralization and pyrite
902 oxidation in groundwater: Importance for silicate weathering in boreal forest soils and
903 stream base-flow chemistry. *Applied Geochemistry* 26: 319–325
- 904 [84] Lovering TS (1959) Significance of accumulator plants in rock weathering. *Bull Geol Soc*
905 *Am* 70: 781– 800.
- 906 [85] Kim J, Dong H, Seabaugh J, Newell JS, Eberl DD (2004) Role of Microbes in the
907 Smectite-to-Illite Reaction. *Science* 303 (830)
- 908 [86] Kurtz AC, Derry LA, Chadwick OA (2002), Germanium-silicon fractionation in the
909 weathering environment. *Geochim Cosmochim Ac* 66: 1525–1537
- 910 [87] Lerman A, Wu LL, Mackenzie FT (2007) CO₂ and H₂SO₄ consumption in weathering
911 and material transport to the ocean, and their role in the global carbon balance. *Mar Chem*
912 106: 326–350.
- 913 [88] Likens GE, Bormann FH, Johnson NM, Fisher DW, Pierce RS (1970) Effects of Forest
914 Cutting and Herbicide Treatment on Nutrient Budgets in the Hubbard Brook Watershed-
915 Ecosystem. *Ecol Monogr* 40 (1): 23-47
- 916 [89] Loucaides S, Behrends T, Van Cappellen P (2010) Reactivity of biogenic silica: Surface
917 versus bulk charge density. *Geochim Cosmochim Ac* 74: 517–530
- 918 [90] Lucas Y, Luizao FJ, Chauvel A, Rouiller J, Nahon D (1993) The relation between
919 biological activity of the rain forest and mineral composition of soils. *Science* 260: 521–
920 523.
- 921 [91] Lucas Y (2001) The role of plants in controlling rates and products of weathering:
922 importance of biological pumping, *Annu. Rev. Earth Pl. Sc.*, 29, 135–163.
- 923 [92] Marschner H (1995) *Mineral Nutrition of higher plants*, 2nd edn. Academic Press,
924 London.
- 925 [93] Mast MA, Drever JI, Baron JS (1990) Chemical weathering in the Loch Vale watershed,
926 Rocky Mountain National Park, [Colorado](#). *Water Resour Res* 26 (12): 2971-2978.
- 927 [94] Matichenkov VV, Bocharnikova EA (2001) In: Datnoff LE, Snyder G H, Korndörfer GH
928 (eds.) *Silicon in agriculture*. *Studies in Plant Science* 8, Elsevier, Amsterdam.
- 929 [95] Madras G, McCoy BJ (2005) Nucleation, growth, and coarsening for two- and three-
930 dimensional phase transitions. *J Cryst Growth* 279: 466–476.
- 931 [96] Massey FP, Hartley SE (2006) Experimental demonstration of the antiherbivore effects of
932 silica in grasses: impacts on foliage digestibility and vole growth rates, *Proc R Soc B* 273:
933 2299–2304
- 934 [97] Markewitz D, Richter D (1998) The bio in aluminium and silicon geochemistry,
935 *Biogeochemistry* 42: 235–252.
- 936 [98] McKeague JA, Cline MG (1963) Silica in soil solutions: II. The adsorption of monosilicic
937 acid by soil and by other substances, *Can J Soil Sci* 43: 83–96.
- 938 [99] Melzer SE, Knapp AK, Kirkman KP, Smith MD, Blair JM, Kelly EF (2010) Fire and
939 grazing impacts on silica production and storage in grass dominated ecosystems.
940 *Biogeochemistry* 97:263–278

- 941 [100] Meunier J-D, Colin F, Alarcon C (1999) Biogenic silica storage in soils, *Geology*
942 27: 835–838.
- 943
- 944 [101] Meunier, J-D, Guntzer F, Kirman S, Keller C (2008) Terrestrial plant-Si and
945 environmental changes. *Mineral Mag* 72: 263–267,.
- 946 [102] Moulton KL, West J, Berner RA (2000) Solute flux and mineral mass balance
947 approaches to the quantification of plant effects on silicate weathering. *Am J Sci* 300:
948 539-570.
- 949 [103] Murphy WM, Pabalan RT, Prikryl JD, Goulet CJ (1996) Reaction kinetics and
950 thermodynamics of aqueous dissolution and growth of analcime and Na-clinoptilolite at
951 25°C. *Am. J. Sci.* 296: 128–186.
- 952 [104] Murnane RJ, Stallard RF (1990), Germanium of silicon of the rivers of the
953 Orinoco drainage basin. *Nature* 344: 749–752.
- 954 [105] Neal C., Jarvie HP, Neal M, Love AJ, Hill L, Wickham H (2005) Water quality
955 of treated sewage effluent in a rural area of the upper Thames Basin, southern England,
956 and the impacts of such effluents on riverine phosphorus concentrations. *J Hydrol* 304:
957 103–117
- 958 [106] O'Brien AK, Rice KC, Bricker OP, Kennedy MM, Anderson RT (1997) Use of
959 geochemical mass balance modeling to evaluate the role of weathering in determining
960 stream chemistry in five mid-Atlantic watersheds on different lithologies. *Hydrol Process*
961 11: 719-744
- 962 [107] Oelkers E. H., Schott J., and Devidal J. L. (1994) The effect of aluminum, pH,
963 and chemical affinity on the rates of aluminosilicate dissolution reactions. *Geochim*
964 *Cosmochim Ac* 58, 2011–2024.
- 965 [108] Oelkers EH, Schott J (1999) Experimental study of kyanite dissolution rates as a
966 function of chemical affinity and solution composition, *Geochim Cosmochim Ac* 63(6):
967 785–797.
- 968 [109] Opfergelt S, Cardinal D, André L, Delvigne C, Bremond L, Delvaux B (2010)
969 Variations of $\delta^{30}\text{Si}$ and Ge/Si with weathering and biogenic input in tropical basaltic ash
970 soils under monoculture. *Geochim Cosmochim Ac* 74: 225–240,.
- 971 [110] Opfergelt S, Delvaux B, André L, Cardinal D (2008) Plant silicon isotopic
972 signature might reflect soil weathering degree. *Biogeochemistry* 91: 163–175.
- 973 [111] Petersen L (1976) In: Hutchinson TC, Havas M (Eds) *Effects of Acid*
974 *Precipitation on Terrestrial Ecosystems*. Plenum, New York.
- 975 [112] Pokrovski GS, Schott J (1998) Experimental study of the complexation of silicon
976 and germanium with aqueous organic species: Implications for germanium and silicon
977 transport and Ge/Si ratio in natural waters. *Geochim Cosmochim Ac* 62 (21/22): 3413–
978 3428.
- 979 [113] Rice KC, Bricker OP (1995) Seasonal cycles of dissolved constituents in
980 streamwater in two forested catchments in the mid-Atlantic region of the eastern USA [J](#)
981 [Hydrol](#) 170 (1-4): 137-158
- 982 [114] Rietra RP, Hiemstra T, Van Riemsdijk WH (2000) Electrolyte anion affinity and
983 its effect on oxyanion adsorption on goethite. *J Colloid Interface Sci* 229: 199–206.
- 984 [115] Robertson FN (1991) *Geochemistry of Ground Water in Alluvial Basins of*
985 *Arizona and Adjacent Parts of Nevada, New Mexico, and California* Washington, D.C.,
986 United States Geological Survey, Professional Paper 1406-C/
- 987 [116] Rajasekaran R, Rajendiran KV, Kumar RM, Jayavel R, Dhanasekaran D,
988 Ramasamy P (2003) Investigation of the nucleation kinetics of zinc thiourea chloride
989 (ZTC) single crystals. *Mat Chem Phys* 82: 273–280.
- 990 [117] Reiners WA, Bouwman AF, Parsons WFJ, Keller M (1994) Tropical Rain Forest
991 Conversion to Pasture: Changes in Vegetation and Soil Properties. *Ecol Appl* 4:363–377.
- 992 [118] Saccone L, Conley DJ, Sauer D (2006) Methodologies for amorphous silica
993 analysis. *J Geochem Explor* 88: 235–238
- 994 [119] Sauer D, Saccone L, Conley DJ, Herrmann L, Sommer M (2006) Review of
995 methodologies for extracting plant-available and amorphous Si from soils and aquatic
996 sediments. *Biogeochemistry* 80: 89–108.
- 997 [120] Savva Y, Szlavetz K, Pouyat RV, Groffman PM, Heisler G (2009) Effects of
998 Land Use and Vegetation Cover on Soil Temperature in an Urban Ecosystem. *Soil Sci*
999 *Soc Am J* 74:469–480
- 1000 [121] Scribner AM, Kurtz AC, Chadwick OA (2006) Germanium sequestration by
1001 soil: Targeting the roles of secondary clays and Feoxyhydroxides. *Earth Planet Sci Lett*
1002 243: 760–770

- 1003 [122] Scanlon TM, Raffensperger JP, Hornberger GM (2001) Modeling transport of
1004 dissolved silica in a forested headwater catchment: Implications for defining the
1005 hydrochemical response of observed flow pathways. *Water Resources Research* 37 (4):
1006 1071–1082.
- 1007 [123] Sfrattore A, Garnier J, Billen G, Conley DJ, Pinault S (2006) Diffuse and Point
1008 Sources of Silica in the Seine River Watershed, *Environ Sci Technol* 40: 6630-6635
- 1009 [124] Smis A, Van Damme S, Struyf E, Clymans W, Van Wesemael B, Frot E,
1010 Vandevenne F, Van Hoestenbergh T, Govers G, Meire P (2011). A trade-off between
1011 dissolved and amorphous silica transport during peak flow events (Scheldt river basin,
1012 Belgium): impacts of precipitation intensity on terrestrial Si dynamics in strongly
1013 cultivated catchments. *Biogeochemistry* 106:475–487
- 1014 [125] Sommer M, Kaczorek D, Kuzyakov Y, Breuer J (2006) Silicon pools and fluxes
1015 in soils and landscapes—a review. *J Plant Nutr Soil Sci* 169, 310–329.
- 1016 [126] Street-Perrott FA, Barker PA (2008) Biogenic silica: a neglected component of
1017 the coupled global continental biogeochemical cycles of carbon and silicon. *Earth Surf*
1018 *Process Landforms* 33: 1436–1457
- 1019 [127] Struyf E, Smis A, van Damme S, Garnier J, Govers G, van Wesemael B, Conley
1020 DJ, Batelaan O, Frot E, Clymans W, Vandevenne F, Lancelot C, Goos P, Meire P (2010)
1021 Historical land use change has lowered terrestrial silica mobilization, *Nat Commun*
1022 1(129) DOI:10.1038/ncomms1128
- 1023 [128] Struyf E, Conley DJ (2008) Silica: an essential nutrient in wetland
1024 biogeochemistry. *Front Ecol Environ* 6, doi:10.1890/070126
- 1025 [129] Struyf E, Conley DJ (2012) Emerging understanding of the ecosystem silica
1026 filter. *Biogeochemistry* 107: 9–18
- 1027 [130] Stumm W, Wollast R, 1990. Coordination chemistry of weathering: Kinetics of
1028 the Surface-Controlled Dissolution of Oxide Minerals. *Rev Geophys* 28: 53-69.
- 1029 [131] Sverdrup HU, Warfvinge P (1988) Weathering of primary silicate minerals in the
1030 natural soil environment in relation to a chemical weathering model. *Water Air Poll* 38:
1031 387-408.
- 1032 [132] Sverdrup HU (1990) The kinetics of base cation release due to chemical
1033 weathering. Lund Univ. Press.
- 1034 [133] Tallberg P, Hartikainen H, Kairesalo T. (1997) Why is soluble silicon in
1035 interstitial and lake water samples immobilized by freezing? *Wat Res* 31(1): 130-134
- 1036 [134] Taylor LL, Leake JR, Quirk J, Hardy K, Banwart SA, Beerling DJ (2009)
1037 Biological weathering and the long-term carbon cycle: integrating mycorrhizal evolution
1038 and function into the current paradigm. *Geobiology* 7: 171–191.
- 1039 [135] Tejedor M, Jiménez C, Rodríguez M, Morillas G (2004) Effect of soil use
1040 change on soil temperature regime ISCO 2004 - 13th International Soil Conservation
1041 Organisation Conference – Brisbane, July 2004 Conserving Soil and Water for Society:
1042 Sharing Solutions
- 1043 [136] Tréguer P, Nelson DM, Van Bennekom AJ, Demaster DJ, Leynaert A,
1044 Queguiner B (1995) The silica balance in the world ocean - A re-estimate, *Science*, 268,
1045 375-379.
- 1046 [137] Van Cappellen P (2003) In: Dove P, DeYoreo J, Weiner S (eds)
1047 Biomineralizations. *Reviews in Mineralogy and Geochemistry* 54: 357-381. Mineral.
1048 Soc. Amer., Washington, D.C.
- 1049 [138] Van Cappellen P, Dixit S, van Beusekom J (2002) Biogenic silica dissolution in
1050 the oceans: Reconciling experimental and field-based dissolution rates. *Global*
1051 *Biogeochem Cy* 16. DOI:10.1029/2001GB001431
- 1052 [139] Vandevenne F, Struyf E, Clymans W, Meire P (in press) Agricultural silica
1053 harvest: have humans created a new loop in the global silica cycle? *Research*
1054 *Communications, Front Ecol Environ*
- 1055 [140] van Hees PAW, Lundström US, Giesler R (2000) Low molecular weight organic
1056 acids and their Al-complexes in soil solution—composition, distribution and seasonal
1057 variation in three podzolized soils. *Geoderma* 94, 2000.
- 1058 [141] Vance GF, David MB (1991) Chemical characteristics and acidity of soluble
1059 organic substances from a northern hardwood forest floor, central Maine, USA. *Geochim*
1060 *Cosmochim Ac* 55 (12): 3611-3625
- 1061 [142] Velbel MA (1993) Formation of protective surface layers during silicate-mineral
1062 weathering under well-leached, oxidizing conditions. *Am Mineral* 78: 405-414
- 1063 [143] Velbel MA (1993) Weathering and pedogenesis at the watershed scale: Some
1064 recent lessons from studies of acid-deposition effects. *Chem Geol* 107: 337-339

- 1065 [144] Wada K (1989) in Dixon JB, Weed SB (eds.) Minerals in soil environments.
1066 SSSA Book series No.1, Madison.
1067 [145] Watteau F, Villemin G (2001) Ultrastructural study of the biogeochemical cycle
1068 of silicon in the soil and litter of a temperate forest, Eur J Soil Sci 52: 385-396
1069 [146] White AF, Brantley SL (1995) Chemical Weathering Rates of Silicate Minerals.
1070 Mineralogical Society of America Short Course 31: 1-22.
1071 [147] White A F (1995) In: Chemical weathering rates of silicate minerals,
1072 Mineralogical Society of America and the Geochemical Society, Reviews in Mineralogy
1073 and Geochemistry 31: 407-460.
1074 [148] Wilding LP, Drees LR (1974) Contributions of Forest Opal and Associated
1075 Crystalline Phases of Fine Silt and Clay Fractions of Soils. Clay Clay Miners 22: 295-306
1076 [149] Woli KP, Hayakawa A, Kuramochi K, Hatano R (2008) Assessment of river
1077 water quality during snowmelt and base flow periods in two catchment areas with
1078 different land use. Environ Monit Assess 137:251-260
1079
1080
1081
1082
1083
1084

1085 List of Figure Captions

1086 **Fig.1:** Classification of Si compounds present in soils. Arrows show increasing stability of solid
1087 compounds against weathering (Sauer et al., 2006; Cornelis et al., 2011).

1088 **Fig. 2:** Estimation procedure for Si concentration in soil water and groundwater by taking into
1089 account dissolution and sink processes. This model is based on equations 10, 14, 16 and 17.

1090 **Fig. 3:** Typical soil profile in temperate climate. Processes and soil moisture vary with depth from
1091 one horizon to another. DSi relative values are estimated for this soil covered by vegetation with a
1092 passive uptake of Si and with important adsorption and precipitation processes in the B horizon.

1093 **Fig. 4:** Conceptual model of the transport of DSi through each horizon. Each box is an horizon
1094 with dissolution and sink processes of different relative importance (thick arrow: important
1095 process). Dashed arrows show the transport from one horizon to another, until the river as final
1096 receptor.

1097 **Fig. 5:** Relative importance of the parameters (B_{Si} , [org], pCO_2 , pH, $[SO_4^{2-}]$, $[CO_3^{2-}]$, θ , r_A)
1098 influencing the DSi concentrations in natural waters of forests (F), grasslands (G) and croplands
1099 (C); parameters influence equations 10 and 12.

1100 **Fig. 6:** Processes influencing the DSi dissolution in soils of forests, croplands and grasslands
1101 during summer and winter, assuming the same soil type for the three cases.

1102

1103

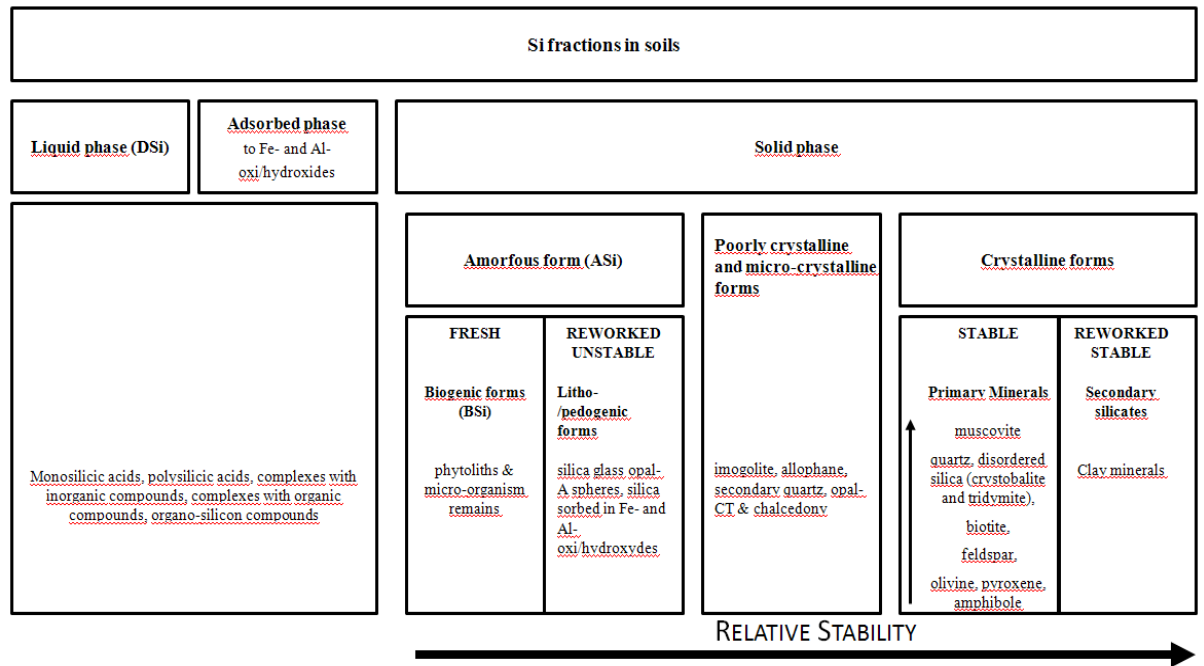
1104

1105

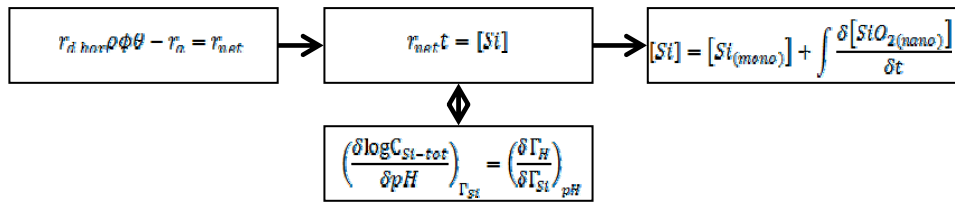
1106

1107

1108 List of Figures



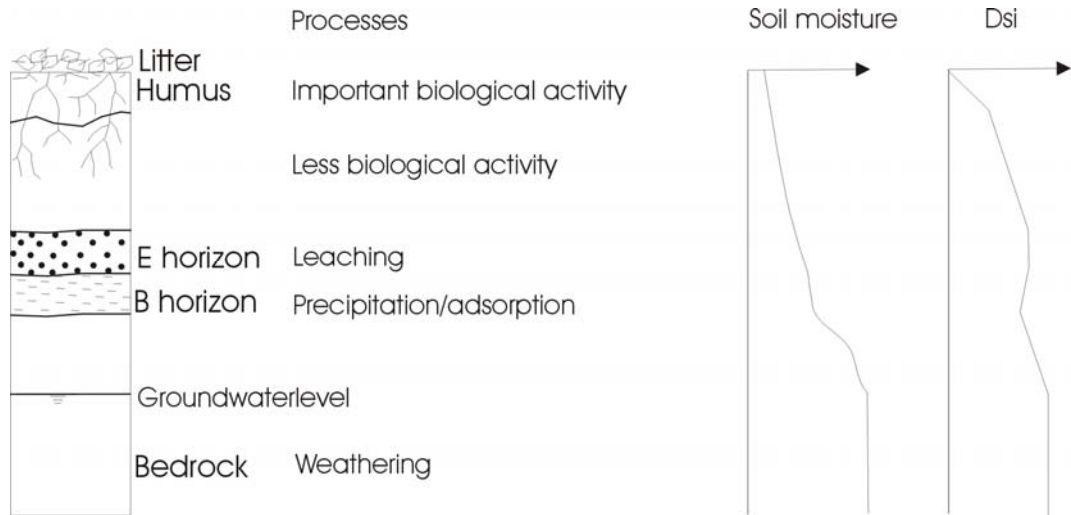
1109 **Fig. 1:** Classification of Si compounds present in soils. Arrows show increasing stability of solid
 1110 compounds against weathering [32, 119].
 1111
 1112
 1113



1114

1115 **Fig. 2:** Estimation procedure for Si concentration in soil water and groundwater by taking into
 1116 account dissolution and sink processes. This model is based on equations 10, 14, 16 and 17.

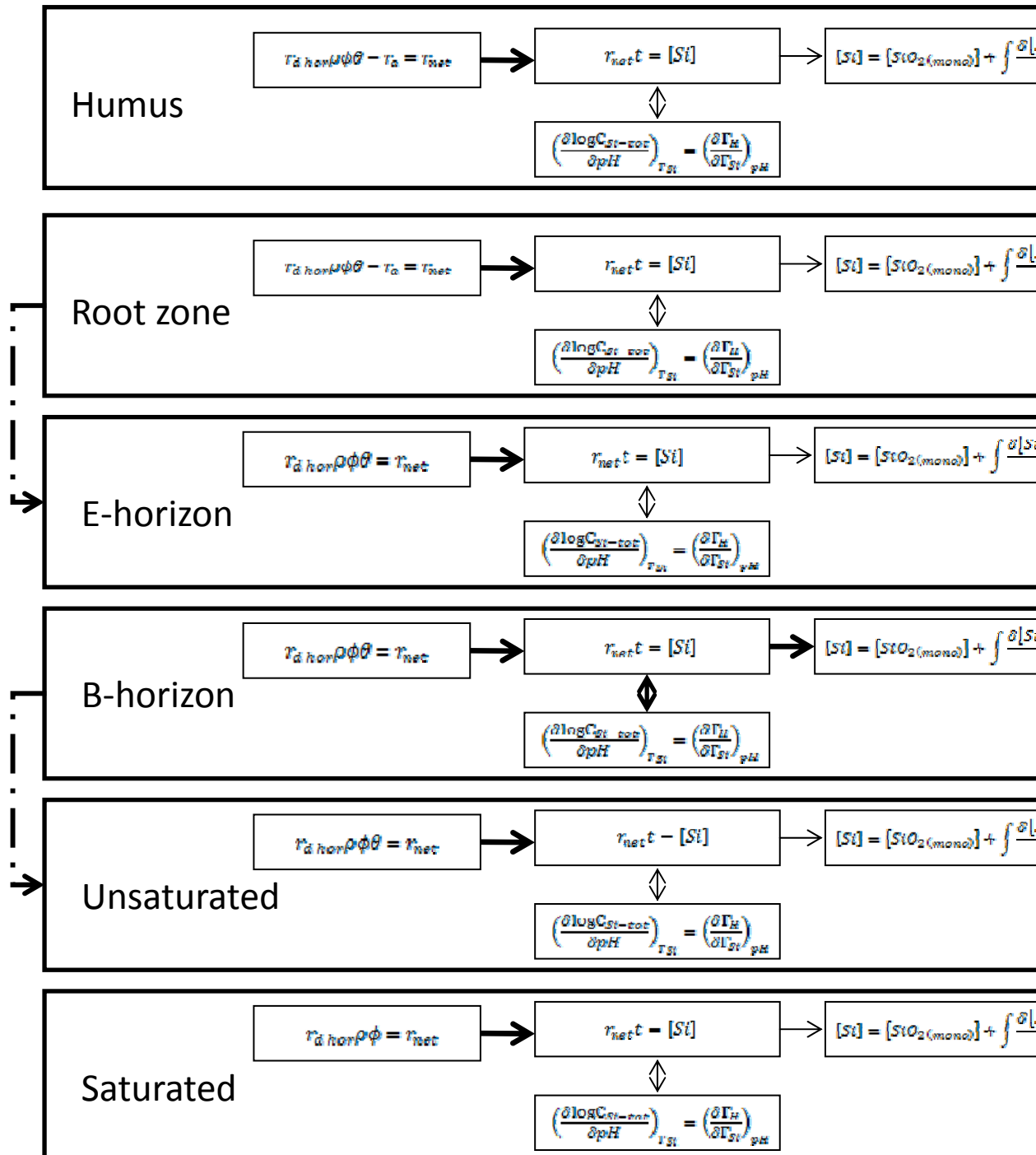
1117



1118

1119 **Fig. 3:** Typical podzol soil profile in temperate climate. Processes and soil moisture vary with
 1120 depth from one horizon to another. DSi relative values are estimated for this soil covered by
 1121 vegetation with a passive uptake of Si and with important adsorption and precipitation processes in
 1122 the B horizon.

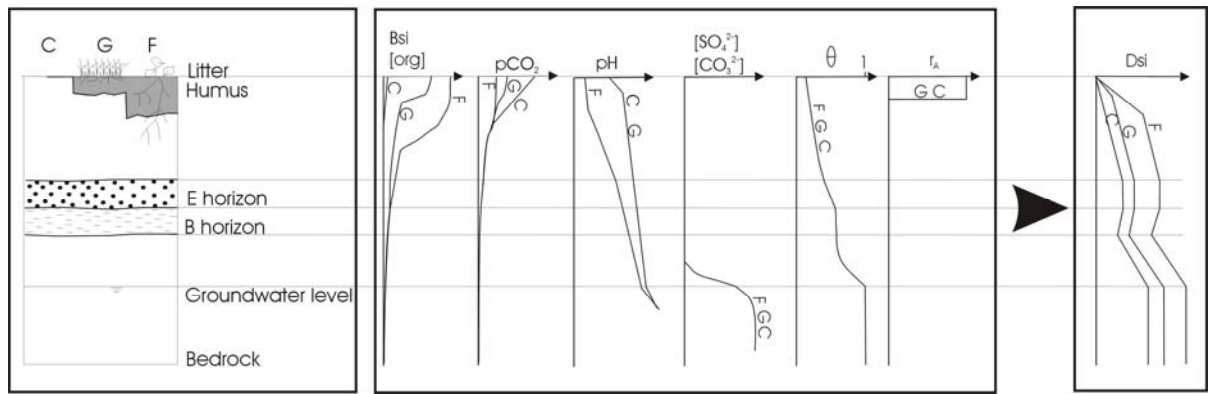
1123



1124

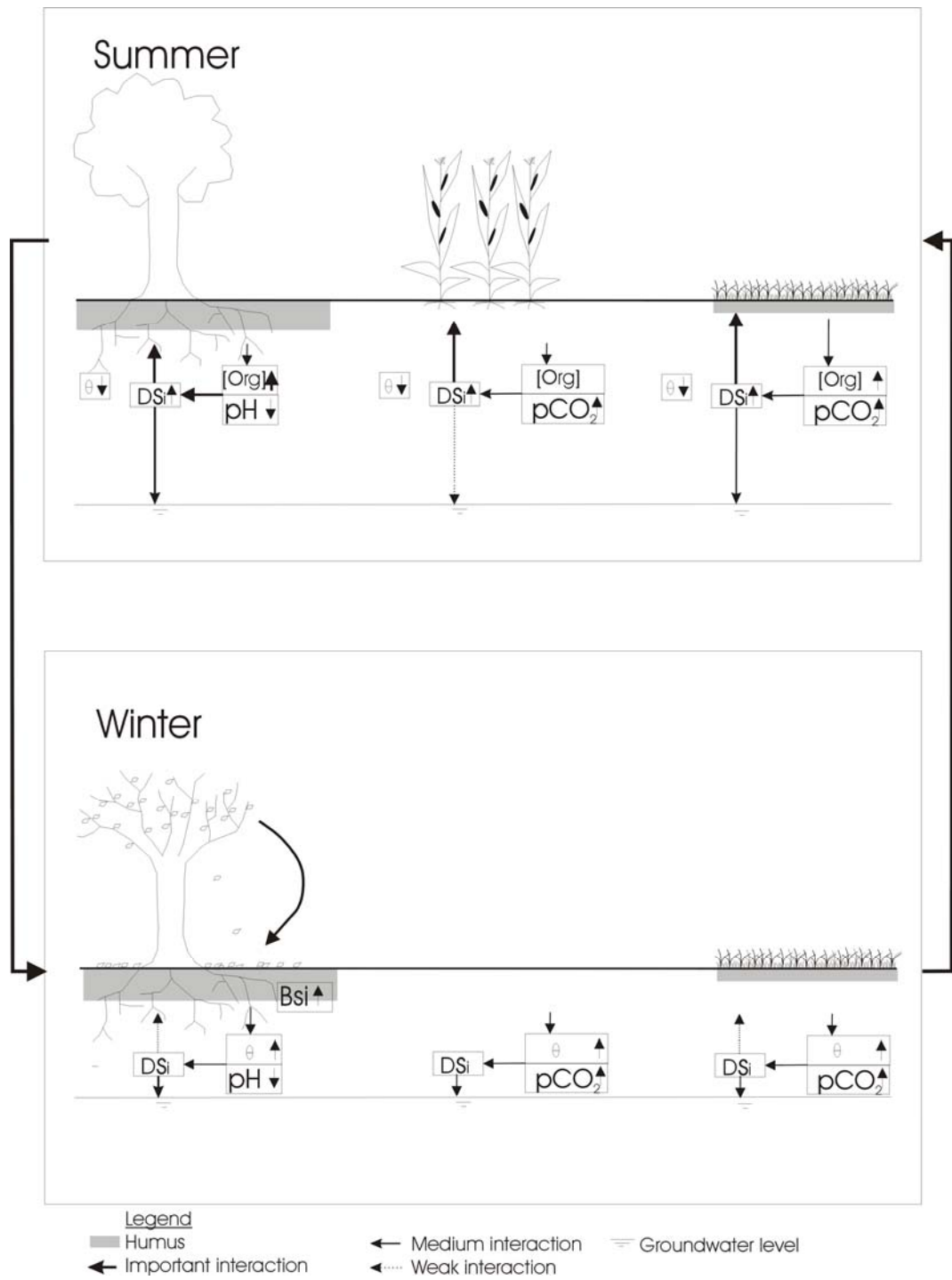
1125 **Fig. 4:** Conceptual model of the transport of DSI through each horizon of a podzol soil. Each box
 1126 is an horizon with dissolution and sink processes of different relative importance (thick arrow:
 1127 important process). Dashed arrows show the transport from one horizon to another, until the river
 1128 as final receptor.

1129



1130

1131 **Fig. 5:** Relative importance of the parameters (BSi, [org], pCO₂, pH, [SO₄²⁻], [CO₃²⁻], θ , r_A)
 1132 influencing the DSi concentrations in natural waters of forests (F), grasslands (G) and croplands
 1133 (C); parameters influence equations 10 and 12.



1134

1135

1136 **Fig. 6:** Processes influencing the DSi dissolution in soils of forests, croplands and grasslands
 1137 during summer and winter, assuming the same soil type for the three cases.

1138

1139

1140

1141

1142 List of Table Captions

1143 **Table 1:** Relative importance of parameters of equations 10, 12 and 17 for each soil horizon for a
 1144 soil profile like presented in Fig. 3. +++, ++, +, ±, - is the scale from very important to
 1145 unimportant. 0 stands for negligible and ϕ for porosity.

1146

1147 List of Tables

1148 **Table 1:** Relative importance of parameters of equations 10, 12 and 17 for each soil horizon for a
 1149 soil profile like presented in Figure 3. +++, ++, +, ±, - is the scale from very important to
 1150 unimportant. 0 stands for negligible and ϕ for porosity.

		r_d					θ	r_a^1
		[H ⁺] ¹	[CO ₂] ¹	[org] ¹	[SO ₄ ²⁻]	[CO ₃ ²⁻]		
Unsaturated	Humus	+++	+++	+++	0	0	< ϕ	±
	A horizon	++	++	++	0	0	< ϕ	±
	E-horizon	+	+	±	0	0	< ϕ	0
	B-horizon	-	±	±	0	0	< ϕ	0
Saturated zone		±	±	±	±	±	ϕ	0

1151 ¹This factor needs to be taken into account if uptake is active and only in the root zone.

1152

1153
1154
1155
1156
1157
1158
1159
1160